Viscoelasticity of the folded domain of a single protein at varying frequencies

VISHAL
BS-MS

Indian Institute of Science Education and Research, Pune
India

May 17, 2024

A thesis submitted to Indian Institute of Science Education and Research,Pune partial fulfilment of the requirements of the degree of
BS-MS dual degree

Abstract

Understanding the mechanics of folded single proteins help us understand several biological processes. One of the established methods is Single-molecule force spectroscopy. The conformational stability of a folded state which allows the protein to adopt different shapes and perform functions can be characterised by its viscoelasticity. Pulling the single protein and observing its nanomechanical response can provide insight into its functioning. We use sequentially arranged 8 domains I-27 the immunoglobulins (IgG) of titin and measure its stiffness and internal friction to understand the mechanics of a folded single protein. We will use a special interferometer-based atomic force microscope for direct and simultaneous measurement of stiffness and internal friction. In addition to this, we will also perform the unfolding of titin (I-27) protein at higher pulling frequencies and micro-sec-time resolution using high-speed force spectroscopy. In this project, we will perform protein unfolding at different frequencies. We will use interferometer-based AFM to pull the protein at different frequencies ranging from 100 Hz to 2 kHz and HS AFM to go further to 100 kHZ. The direct measurement of stiffness and friction of folded states has been recently established using special interferometer-based AFM but not at several ranges of pulling rates and frequencies. We will compare the data we get from interferometer-based AFM and high-speed AFM. The aim of this project is:
1. Directly measuring the stiffness and internal friction of folded states of single protein at ranging frequencies.
k 2. Comparing the results of protein pulling of interferometer-based AFM and high-speed AFM.

Certificate

This is to certify that this dissertation entitled "Viscoelasticity of the folded domain of a single protein at varying frequencies" towards the partial fulfilment of the BS-MS dual degree programme at the Indian Institute of Science Education and Research, Pune represents study/work carried out by "Vishal at IISER Pune and AMU, Marseille France)" under the supervision of Dr. Felix Rico, Associate Professor at Aix-Marseille Université-Inserm-CNRS and Dr. Shivprasad Patil, Professor at Department of Physics, IISER Pune during the academic year 2023-24.

Dr. Felix Rico
Project Supervisor
Aix-Marseille Université-Inserm-CNRS

Committee:
Prof. Felix Rico
Prof. Shivprashad Patil
Prof. Apratim Chatterji

Declaration

I hereby declare that the matter embodied in the report entitled “Comparison of viscoelastic measurements by High speed and Interforometer-based AFM ” are the results of the work carried out by me at the Department of Physics, A thesis submitted to the Indian Institute of Science Education and Research, Pune and Aix-Marseille Université-Inserm-CNRS, under the supervision of Dr Shivprasad Patil and Dr Felix Rico, the same has not been submitted elsewhere for any other degree.

Signature of Student: 

Vishal

May 17, 2024

Acknowledgements

I would like to acknowledge my Supervisors, Dr Shivprasad Patil and Felix RICO, for their academic and social support. They both always were very friendly and approachable to me in times of need. I had a lot of freedom to choose the problem of my interest and explore the instruments and resources available in the lab. I have always been inspired and fascinated by such personalities who work so hard, have achieved so much and still maintain a cool personality.

I am thankful to all my lab members from both labs with whom I had a lot of fun and who supported me and helped me in my project, social life, and even sometimes financially. My colleagues Swarnavo, Mayank, Danny, Claire, Eider and Yogesh have greatly helped me during the MS thesis. A special thanks to Shatruhan Bhaiya because of whom I got stuck in the field of AFM in the first place. I am grateful that he has always kept an open heart, encouraging tone, friendly behaviour and a charming smile in the time of need.

I thank all my IISER friends for making my life in IISER so adventurous. Thanks to my online study group Sakshi Ve, Suyash, Mahima, and Anitha, even after being so far apart, we have always remained entangled through technology.

I love you Mamiji, Papaji, without whom none of this would have been possible. I won't ever forget those tears of happiness in my Papaji's eyes when I got admission to IISER. You always have let me choose for myself, always have supported me and encouraged me on every small to big step.

Contents

List of Figures

List of Tables

Part I

Introduction

1

Introduction

1.1 Proteins

Proteins are essential building blocks of all living organisms across various kingdoms. These macromolecules play vital roles in DNA replication, metabolism, inter and intra-cellular communication, transportation of molecules and organelle, cell adhesion, cell division/degradation, cell and tissue structure maintenance, mechano-transduction, and immune system response. Hence, the study of the fundamental properties of proteins becomes crucial in understanding different biological processes and is helpful in curing many diseases. Once the formation and functions of proteins are understood.

These proteins perform their function by changing their conformations. The change in conformation can be due to various environmental factors, such as changes in pH and temperature or under an applied force. There is a strong correlation between their structure and function, which leads to such conformal changes. There are a variety of proteins that work under forces. The mechanical properties of such proteins are essential to understand their function. The mechanical properties of these proteins are essential to understand their functions. Various techniques have been developed to investigate their mechanical properties, such as Atomic Force Microscopy(AFM), Optical Tweezers and Magnetic Tweezers. In this chapter, I will briefly introduce proteins, their function, formation, and different applications in the human body. I will also discuss the technique used to investigate the thermodynamics and kinematics of protein folding and unfolding in detail. These

techniques include studying protein in bulk and single molecule levels. The focus of my discussion will be single-molecule force spectroscopy using AFM.

1.1.1 Protein structure

Proteins are polymers of amino acids. They are also known as polypeptides, which are made of monomer units of amino acids. Amino acids are organic compounds containing the amine group (NH_2) and the carboxylic group (-COOH). Each amino acid features a central carbon atom bonded to an amine group, a carboxyl group, a hydrogen atom, and a unique side chain (R group). This R-group characterizes the amino acid. For the polymerization of amino acids to protein, the carboxylic group of one amino acid reacts with the amine group of another amino acid, releasing H_2O in the process (dehydration). The product of this dehydration reaction is a dipeptide (fig. 1.1) with two amino acids bound with a peptide bond (C-N). The dehydration process continues, adding new amino acids to the chain, forming a *polypeptide* chain. The end with $-NH_2$ group is called the N terminus and -COOH is called the C terminus of the protein. This polypeptide chain is known as the protein's primary structure. All amino acids are attached with covenant bonds in their primary structure. As the length of the polypeptide increases, this primary structure can bend and fold into regular patterns, such as alpha helices and beta sheets. These patterns are stabilized by non-covalent bonds between the amino acid backbones, such as hydrogen bonds, Van der Waals force etc. These interactions and the higher structures depend on the amino acids' variety and sequence. The secondary structure is categorized mainly in two parts on the basis of their arrangement:

- α-helix: A right-handed coil stabilized by hydrogen bonds between one amino acid's carbonyl group and another amino acid residues ahead. Each of these α-helix contains 3.6 amino acids.

- β sheet: Two or more polypeptide chains align side-by-side, forming hydrogen bonds between their backbones. These sheets can be arranged in parallel or antiparallel. configurations

These secondary structures fold upon themselves in a unique 3D arrangement known as the *tertiary structure*. Again 3D structure is maintained by non-covenant interactions such as H-bonds, ionic bonds, disulfide bonds (-SH), and hydrophobic interactions. Some proteins consist of multiple polypeptide chains assembled into a single functional unit, forming the *quaternary structure* e.g. Hemoglobin.

1.1.2 Protein Classification

There are thousands of different proteins in our body, each having a different function. The function a protein performs depends on its structure and conformation. It is essential for the protein

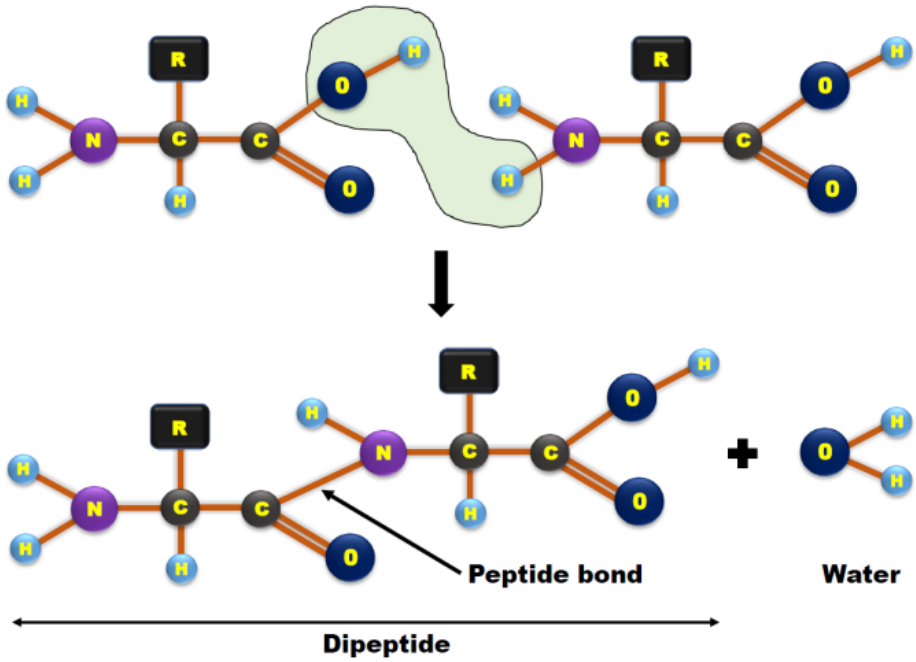

Figure 1.1: Amino acid contains amine group(NH_2) and carboxlyc group($COOH$). The figure represents the formation of peptide bond between two amino acids by dehydration(release of H_2O) and fo. By the same process multiple amino acids can react and form a polypeptide in its primary structure.

to change its conformation and acquire the desired structure in order to perform its specific task. If it does not acquire the specific conformation, then it is said to be *misfolded*. These changes in conformation depend on the interaction of the protein with its environment. On protein's structure and interaction, the protein is mainly of three types:

Globular Proteins: The globular proteins are folded in such a manner that their hydrophobic side is buried deep within their body. They take a spherical shape and are water-soluble. Due to their water solubility, they freely move inside the cell and perform various functions, such as the transportation of other molecules, such as enzymes and antibodies. Interestingly, many of the fibrous proteins are made up of globular proteins, e.g. the muscle protein has Ig domains, which are globular proteins. A few other examples are haemoglobin, insulin, and antibodies.

Fibrous proteins: Fibrous proteins are made up of polypeptide chains arranged in a parallel axis. They are built up into long fibres or large sheets. They are typically very strong and hydrophobic. They play the role of structural proteins, providing mechanical stability and support. Examples include collagen (in skin and bones), keratin (in hair and nails), and elastin (in skin and ligaments).

Membrane proteins: The cell membrane separates the cell from its environment. This membrane is made of lipid bilayer. The membrane proteins are embedded in the cell membrane and organelles inside the cell. They help transport molecules across the membrane. Some of the examples are aquaporins (water channels) and ion channels.

1.2 Unfolding of protein

There is a strong relation between the structure and function of the protein. The function of protein is the 3D structure it attains in the environmental condition. The 3D structure depends on all the different amino acids that make it up. To get a complete picture of the understanding of the proteins, we have to answer three major questions: (i) How does the protein attain its primary 3D structure? (ii) How Does the protein change its conformation/ perform folding and unfolding? (iii) How does the protein avoid misfolding?

Several earlier studies have used different methods to unfold the protein. The protein is denatured in these experiments, and some observable parameters are recorded under different reaction coordinates. These studies are either *Bulk Studies* or *single molecule studies*. In Bulk studies, the average behaviour of the proteins is observed. The unfolding can be caused by different methods, such as increasing temperature, applying pressure or dissolving in some denaturation agent(e.g. urea). The protein is directly investigated under different experimental conditions in single molecular studies. Unlike bulk studies, we can study local and small features in single-molecule experiments, such as measurement of the intermediate state of the protein unfolding process. In past decades, many techniques for the measurement of single molecules have been developed. These techniques can be

mainly classified into two categories: single-molecule fluorescent microscopy and single-molecule force spectroscopy.
In Single-molecule fluorescent spectroscopy, a fluorescent molecule is attached to the molecule(protein) and observed under a specific wavelength laser. By focusing a laser beam on the sample and using highly sensitive detectors, fluorescence emitted by individual molecules can be detected.
Another powerful technique in single-molecule studies is single-molecule force Spectroscopy(SMFS). Various studies have investigated the thermodynamic and kinematic properties of single molecules[5, 7, 12]. In SMFS, the unfolding of protein is observed by applying external force onto it. Three major methods widely used for applying forces on single molecules are Optical tweezers, Magnetic tweezers and Atomic force microscopes. The Optical tweezers provide the most sensitivity among these methods [18]. This technique traps a bead under a focused laser(optical trapping). The trapped bead acts like a small spring. Proteins and other molecules can be attached with the bead on one end, and force can be applied to the molecule while the other end is kept stable. Optical tweezer can apply forces of the order of a few pN. Another technique for studying the mechanical properties of biomolecules is using magnetic tweezers, which use superparamagnetic beads in a controlled magnetic field. Another widely used tool for single-molecule force spectroscopy (SMFS) experiments is the atomic force microscope (AFM). AFM is the main technique that I used in this project, so I will discuss it in detail in a later section.

1.2.1 Principle behind Atomic Force Microscopy

Atomic force microscopy (AFM) is a type of Scanning probe microscopy(SPM). This technique was first invented by Gerd Binnig, Calvin Quate, and Christoph Gerber in 1986. The precursor to the AFM, the scanning tunnelling microscope (STM), uses quantum tunnelling phenomena to probe the conductive surfaces, and it is performed under ultra-high vacuum (UHV) conditions. But AFM does not require any such conditions. In Atomic force microscopy, a sample is probed under a microscopic cantilever, and the interaction between the sample under study and the cantilever tip produces some deflection in the cantilever 2.4. This deflection in the cantilever can be measured using different techniques, such as using a laser or an interferometer. This technique can be used on a diverse variety of samples, including organic, inorganic materials, conducting or non-conducting, and living samples such as cells. The AFM experiments are modified for various conditions, such as in a liquid medium, air or ultra-high vacuum. In different modes, AFM can be used for various purposes. It is widely used as an imaging tool that can provide 3D topography of surface elasticity, viscoelasticity of material can be used as a force manipulation tool to measure surface properties. Depending on the setup, the resolution of an AFM can be a few nm laterally and a few Å in imaging and pN in force spectroscopy experiments. For a slight bending in the cantilever δ, the stress applied due to the interaction can be estimated using Hook's law $F = k\delta$, where is the force

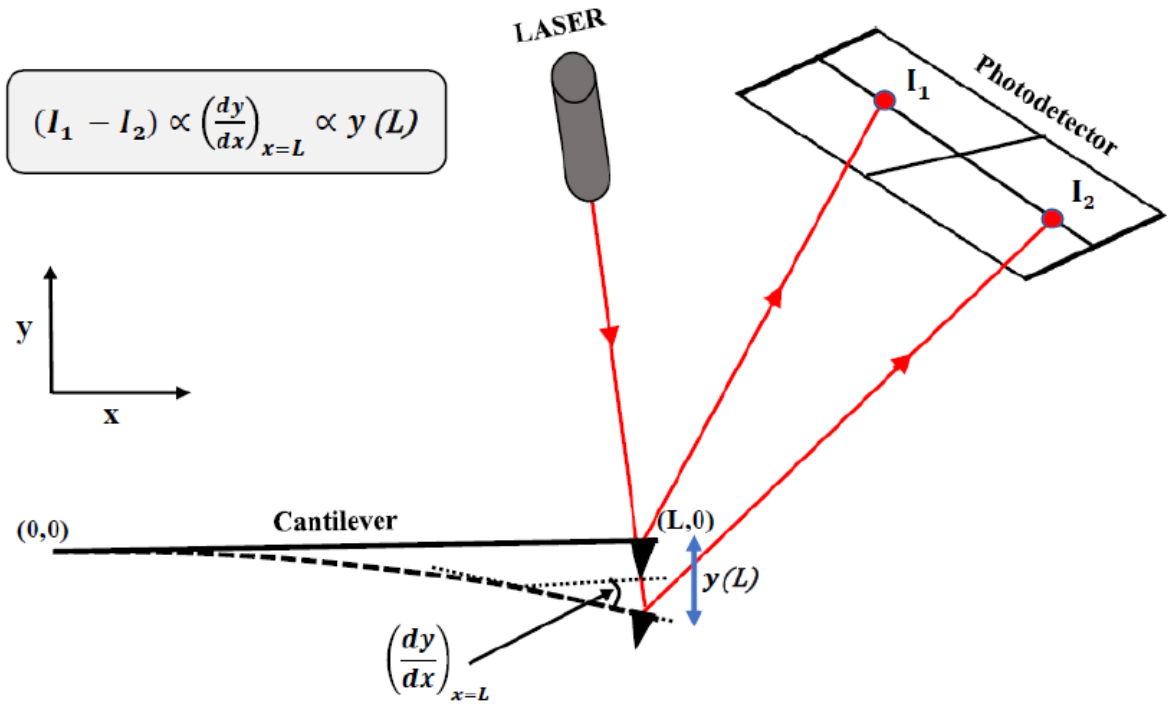

Figure 1.2: Schematic shows how the laser position changes on the photodetector due to the deflection in the cantilever. This deflection can be measured by proportionality $\frac{dy}{dx}\alpha(I_1 - I_2)$ of the four quadrant photo detector.

constant of the cantilever. Typically, the deflection signal of the cantilever is measured in volts, and then this signal is converted into nm using the sensitivity coefficient. Then, the cantilever is calibrated to get the spring constant using different methods. For example, when using a laser to measure the deflection of the cantilever, as shown in 1.2 a slight deflection in the cantilever causes a change in the position of the laser spot on the four-quadrant photo-detector. The change in the laser's position can be calculated by subtracting the upper half detector signal from the lower half, and lateral deflection can be calculated by subtracting the right half detector signal from the left half. In the figure, the deflection of the cantilever $\frac{dy}{dx}$ is proportional to $I_1 - I_2$.

1.2.2 Force spectroscopy Experiments using AFM

One of the most widely used applications of AFM is measuring mechanical properties applying force by micro-cantilever, known as *Force Spectroscopy*. These measurements can be in *Static Mode* or *Dynamic mode*.

Static mode SMFS: In Static mode, also known as *contact mode*, a protein is attached from one end with the cantilever tip and the other end to the sample surface either with *specific binding*

or *unspecific binding*. It is pulled with a constant velocity or is kept at a constant force. For constant speed, the force vs extension(fig 1.3) in the protein curves is obtained, and this is known as constant speed pulling. In the case of constant force, it is known as the force clamp experiment, and the protein's extension is recorded. Both techniques are widely used to investigate the protein's mechanical, kinematic and thermodynamic properties[3, 10, 12, 27]. In these studies, the cantilever is modelled using Hook's law. The force in the cantilever is proportional to its deflection for small deflections in the cantilever. Figure 1.3 shows a typical static mode SMFS experiment; herein (I), a polyprotein attached to the tip from one end cantilever from another it is pulled with constant velocity, and the cantilever deflection is measured using the photodetector in (ii) due to the force applied by the cantilever the domains of the ply protein unfold one by one. (iii) Corresponding to each unfolding in (ii) we can see the peaks in Force vs extension curve.

1.2.3 Force Spectroscopy on Proteins

In the AFM force spectroscopy experiment, the attachment of the protein from the cantilever and the surface is either non-specific(no linkers used for the attachment) or some Poymer linkers bind the ends(N and C- terminus) of the proteins with some specific binding. The protein has a two-state energy landscape with an energy barrier between them (transition state TS); when force is applied to such protein, their energy landscape tilts and lowers the barrier energy, in turn increasing the probability of unfolding.

After unfolding, it loses all the native interactions. Applying further force on the unfolded protein reduces its entropy. Hence, the protein has an excess to less number of conformations. Due to the reduction of the entropy, the protein exerts an entropic force on the cantilever. This was first derived by Marko Siggia with Worm Like Chain (WLC) model[17] and later validated by Bustamante [6].

Worm Like Chain model:

The minimum length scale or *persistance length* of the WLC model is the shortest among other models describing polymer behaviour. That means the correlation of a component dies out very quickly along the polymer length. The relation between the force and extension in WLC is given by:

$$F(x) = \frac{k_B T}{p}\left(\frac{1}{4(1-x/L_c)^{-3}} - \frac{1}{4} + \frac{x}{L_c}\right) \tag{1.1}$$

where L_c, p are contour length and persistence length, k_B, T are the Boltzmann constant and absolute temperature and x is the extension in the polymer.

1.2.4 Models for protein unfolding

Bell-Evans-Ritchie model: This model was first developed by Bell[2] as a model for of cells to cells adhesion; later, this model was adapted to explain the *dynamic strength of molecules* by

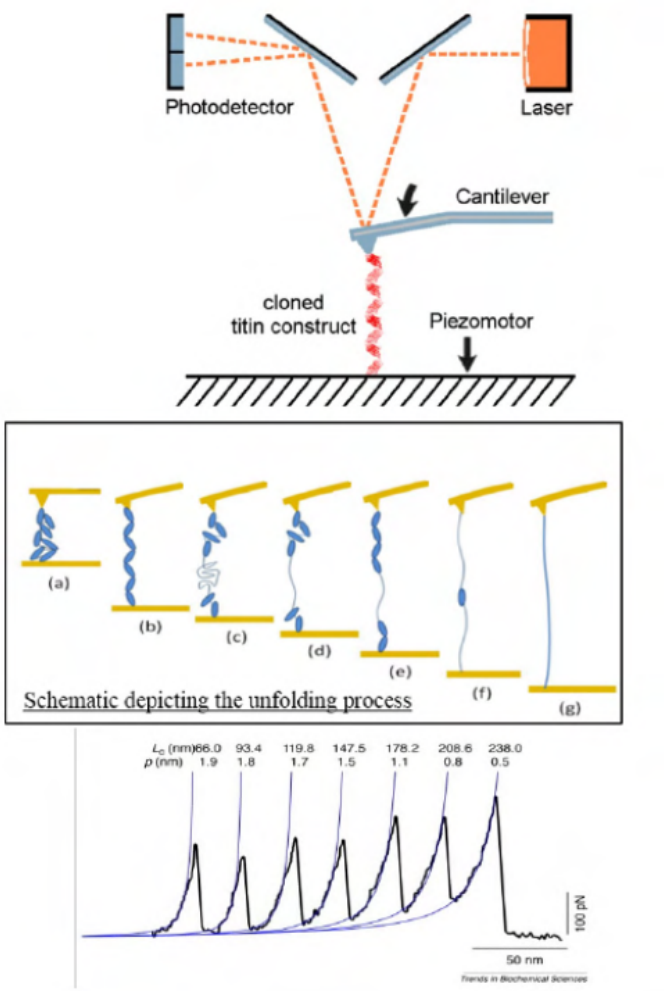

Figure 1.3: Figure shows typical static mode SMFS experiment using AFM; (I) Protein attached to the tip from one end cantilever from another. (ii) From (a) to (g) Unfolding of many domains of the attached protein. (iii) Peaks in the extension corresponding to each unfolding even in (ii)

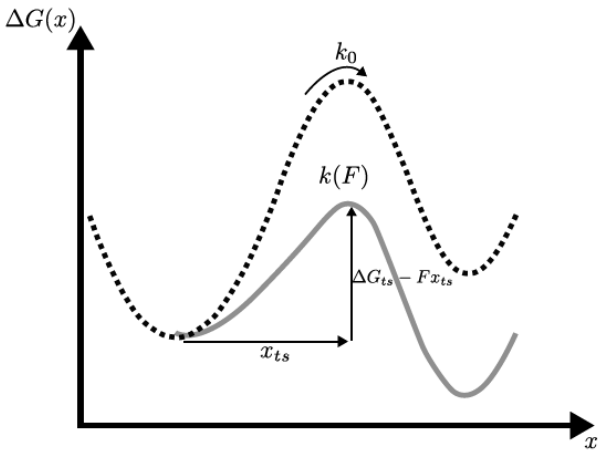

Figure 1.4: Figure: Dotted line shows energy landscape of a protein having transition barrier ΔG_{ts} at x_{ts} in between its two states When a force F is applied on the protein, the energy profile tilts and the barrier reduces to $\Delta G_{ts} - Fx_{ts}$

k_0 is the initial unfolding rate and $k(F)$ is the unfolding rates when force F force is applied..

Evans and Ritchie[9]. According to this model, the rate of unfolding a protein having an energy landscape similar to that of fig 1.4 is given by:

$$k_0 = Aexp(-\Delta G_{ts}/k_BT) \tag{1.2}$$

Where $A = \frac{(\omega_0 \omega_{ts})}{2\pi\gamma}$ depends on the protein's energy landscape and the damping experienced by the protein. When a force F is applied, the energy landscape tilts and increases the unfolding rate as:

$$k(F) = Aexp(-(\Delta G_{ts} - Fx_{ts})/k_BT) \tag{1.3}$$

$$k(F) = k_0 exp(-Fx_{ts}/k_BT) \tag{1.4}$$

Bell-Evans-Ritchie model is used to predict the unfolding at lower loading rates, but it fails at higher loading rates [22].

1.2.5 Viscoelasticity of folded protein

As discussed earlier, proteins are biomolecular machines. They are constantly moving and changing their structure in order to perform their function. The ability to change their structure is a critical factor for function. For example, myoglobin changes its conformation to capture and release O_2. So, to understand the protein's function, it is crucial to understand the protein's mechanical properties. The stiffness and the internal friction are key parameters that characterize the mechanics of the protein. The stiffness of the protein is quantified by performing a force spectroscopy

experiment on the protein by measuring the extent of deformation under force. The internal friction can be quantified by measuring energy dissipation during motion within the rugged energy landscape.

1.2.6 Stifness measurements of Protein using AFM

Typically, in AFM measurements, unfolding force is measured using force-extension curves. The unfolding forces can be used to estimate energy landscape parameters using the Bell-Evans-Ritchie model and the stiffness(k) of protein is measured.[24]. Wang and Zocchi used a different approach; they measured the strain response of the domains of Guanylate Kinase by applying oscillatory stress.[29, 30]. They applied the Maxwell model to the protein domains, meaning they represented the domains with spring and dashpot in series. They attached proteins between two gold nanoparticles, oscillated them, and found the stiffness 5 pN/nm and damping coefficient of the order of 10^{-5} kg/s. However, the experiment was a bulk study, not on a single molecule. Hence, many rheological models can describe the mechanical behaviour of the protein. One of these models is Kelvin–Voigt, which describes the behaviour of a material with a spring and dashpot attached in parallel.

Kelvin voight model

This model is used for materials that behave more like solids than fluids. The material is represented as a spring(E) and a dashpot(η) attached together in parallel. The spring represents the material's stiffness, and the dashpot represents the viscosity(fig. 1.5). The following equation defines the stress-strain relation in this model:

$$\sigma = \eta\ddot{\varepsilon} + E\varepsilon \tag{1.5}$$

where σ is the stress and ε is the strain across the system. The mechanical response of the kelvin-Voight model when oscillatory rheology is performed:

$$G(\omega) = G_0\left(1 + \frac{i\omega\tau}{1 + I\omega\tau}\right) \tag{1.6}$$

If the spring and the dashpot are in series, it is called the Maxwell model.

1.2.7 Dynamic AFM on proteins

As discussed earlier, the internal friction of protein can be measured by performing oscillatory rheology on the protein and measuring the dissipated energy due to oscillations. Therefore, we must apply sinusoidal stress to a single-folded protein and compute the phase lag caused by energy dissipation to determine the protein's viscoelasticity. So, it is very important to measure artefact

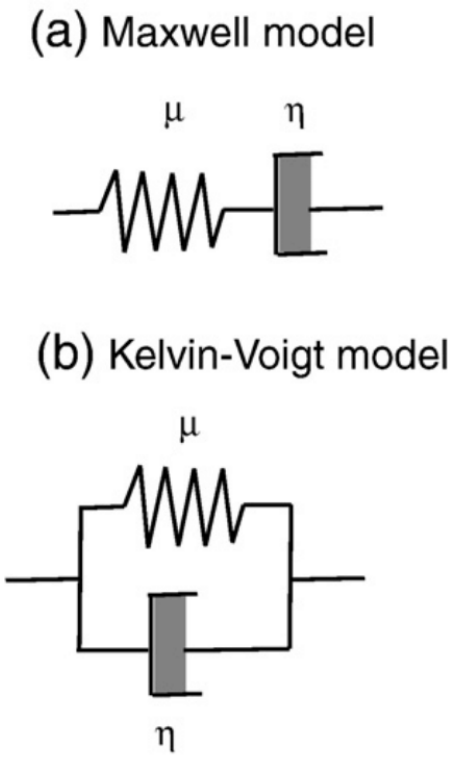

Figure 1.5: Representation of Maxwell model and Kelvin Voight model (a) and (b) respectively. In Maxwell model the spring and the damper are attached in series, In case of Kelvin Voight model the are attached in parallel.

free the amplitude and phase lag of the cantilever's response. The quantification of amplitude and phase lag becomes difficult because of the challenges faced when correctly quantifying the dynamics of the cantilever. Near resonance phase lag and false peaks are observed. This can be solved when the cantilever tip is excited directly using photothermal or magnetic methods(discussed in later chapter.) So, for successfully measuring the viscoelasticity of the protein, off-resonance, with small amplitude measurements, is suggested [16, 8]

1.3 Titin I27

Titin is the largest known polyprotein(m.w. $\sim$ 3MDa, size $\sim$ 1 μm). Titin if found in cardiac and skeletal Muscles. The I-band of titin is responsible for the passive elasticity of the muscles. The I-band of titin comprises mainly two tandem immunoglobulin-like(Ig) segments with a small PEVK segment. There are 200 IG domains in the I-band. I27 is one of those IG domains. The I27 domain is unique to cardiac muscle. It is a β-sheet structured globular protein with seven β-strands and 89 amino acids(fig 1.6)[15]. The titin is widely studied in AFM experiments. The well-defined unfolding behaviour of titin makes it a useful model system for my research into protein mechanics. The I27 homo-polyproteins exhibit a distinctive "sawtooth" unfolding pattern, as demonstrated by AFM investigations. There is an intermediate state to the unfolding of titin, which starts to occur at forces $>$ 95 pN. Once the domain unfolds completely, it adds 0.66 nm to the unfolded chain.

1.4 Motivation and Objective

Proteins are a vital bio-machinery in the human body, and it is essential to understand their structure-function relation. This can help us to synthesize proteins and/or cure many diseases. Due to technical advancements in tools like NMR and electron microscopy, we understand the protein's ensemble-averaged structure. But it is a dynamic molecule; it changes its conformation to function. So, to better understand the protein, we need in-depth information about its mechanical properties. Over decades, using force spectroscopy experiments, new tools and techniques have emerged to study the mechanical properties of biomolecules, such as AFM and optical and magnetic tweezers.

Recently, the viscoelastic behaviour of a single protein has been measured using Interferometer-based AFM via dynamic force spectroscopy experiments [8]. It was done for frequencies from 400 Hz to 2 KHz. The study shows the protein I27 having a transition state between its native and unfolded state

High-speed AFM allows us to go beyond these frequencies and speeds. We can see how the viscous and elastic response changes over frequencies ranging from 2 kHz to 100 kHz and make some observations by the results. The method to measure the viscoelasticity by interferometer-

Figure 1.6: Figure showing seven β-strands of titin I27 molecule. source: (`https://www.rcsb.org/structure/1TIT`)

based AFM is well developed [8]. I want to find a method to measure the same on High-speed AFM and compare the results with those that of already been calculated.
So my objectives of this project are as follows:

1. Perform experiments on Interferometer Home-built AFM and calculate the viscoelasticity with the already established model of dynamic force spectroscopy.

2. Perform dynamic force spectroscopy experiments in High-speed AFM at much higher frequencies(2-100 kHz).

3. Eshtablsih new method to calculate the viscoelasticity from the data

4. Compare the two data to conclude the result.

1.5 My work

We have to perform dynamic force spectroscopy experiments on the proteins to measure the viscoelastic behaviour of the I27 protein at different frequencies. For this the polyprotein of I27 (x8domains) was purified from the plasmids. I have chosen a robust way of immobilising the protein on the sample surface and pulling it from a specific site using the interaction of cohesinIII/dockerin. Functionalization of the protein provides repeatability of experiments and fixes the reaction coordinate for each pulling event.
My work was a collaboration between the lab of Dr Shivprasad Patil, IISER Pune and Dr Felix RIco, Aix Marseille University. In the first three months of my project period, I worked with Dr Patil to repeat the results of viscoelastic measurements done earlier[8] and later, with Dr Rico, I would do dynamic force spectroscopy on the same protein at higher frequencies using High-Speed AFM. My main goal of this thesis is to devise a way to calculate the viscoelasticity of the folded domain of a single protein at higher frequencies.
To measure the viscoelasticity of the folded protein, we have to calculate the energy dissipation of the protein when sinusoidal stress is applied to it. Due to the protein interaction, the strain response of the protein changes its amplitude and phase. The protein is modelled as a simple Kelvin Voight model. The equations of Kelvin Voight's model are solved to calculate the effective stiffness(k) and internal friction(γ). But to achieve this, we need to measure artefact-free amplitude and friction. Hence, we suggest doing the small amplitude off-resonance measurements. Interferometer-based AFM has a great advantage in the small amplitude off-resonance regime as it measures the displacement of the cantilever rather than the deflection, which will be very small. In interferometer-based AFM we use lock-in amplifier which us the change in phase and amplitude which are the observables of the experiments. These observables are then used in the calculation of

viscoelasticity. Similarly, we will have to calculate the amplitude and phase change of the applied oscillations and the stress response to calculate viscoelasticity.

2

Methods and Materials

2.1 Protein purification and Functionalization

Titin is the larges known polyprotein(m.w. $\sim$ 3MDa, size $\sim$ 1 μm). The I-band of titin is responsible for the passive elasticity of the muscles. The I-band of titin comprises mainly two tandem immunoglobulin-like(Ig) segments with a small PEVK segment. There are 200 IG domains in the I-band. I27 is one of those IG domains. It is a globular protein with 89 amino acids.[15] It has seven β-strands. It is well-studied in the literature, and that is why we are choosing it as a standard for comparing our results.
We want to do the specific pulling of the protein for our experiments. This means we want to immobilise the protein from a specific site (N or C terminus) to the surface and pull the construct from another construct with the cantilever. Our construct has 8 repeats of titin I27 domain with dockerin complex covalently immobilized via ybbr peptide. The 8 domains were cloned with ybbr tag at the N-terminus and dockerin at the C terminus. On Cantilever cohesin III is attached via maleimide and APTES. The cohesin III/dockerin bond formation is used for the specific pulling of the protein.

Purification of Protein

Protein, one of the most singular fundamental components of the cell, is periodically synthesized through translation via ribosomes of the functional genetic code of any living cell, the messenger RNA. Hence, it should come as no surprise when we can excruciate the same process

for an independently expressing plasmid by utilizing a cell's translational machinery at a time in synchrony with the cell's own translation period. This is exactly what we did with our vector(PET28a(+)) containing our protein of interest as a gene, which can be accommodated into a translational reading frame (see Vector Diagram for more specifics) with the gene's very own start and stop codon. This was done until the protein was expressed in plentiful amounts within the cell so as to ease further the process of the protein's actual biochemical purification.

Expression System

For this purpose, the host was chosen as the BL21 DE3 E. coli cells, which are prokaryotic in nature were perfect for accommodating our expression vector PET28a (A prokaryotic expression vector), which expressed one particular domain (I-band repeat number 27) of a eukaryotic protein, Titin in 8 consecutive homologous repeats, that didn't require any post-translational modifications to fold correctly into it's native state. Our host of choice had very low codon bias, i.e., its transfer RNAs didn't have rare anticodons against our gene.

Protein Expression and Purification

- Following the "Heat shock" protocol, our plasmid was transformed into the BL21 host and then incubated in an incubator at 37 C for a few hours to recover.

- Aseptic culture transfer was performed periodically from the tube to Luria Broth agar plates so as to get isolated pure cell culture. This was done along with adding the Antibiotic against which our plasmid is resistant (Kanamycin in the case of Titin) to ensure any foreign bacteria and even untransformed cells couldn't survive and show up in the culture.

- This culture was then transferred into a pretty large 1 ml Luria Broth and then transferred into the incubator for the growth of the cells. They were grown until their O.D 600 (Optical Density at 600 nm) reached 0.6 (the late log phase of the bacterial cells). At that stage, they were induced with IPTG (Isopropyl-β-D-thiogalactopyranoside), which basically induces the transcription of our gene of interest and its subsequent translation to the protein of interest.

- The expression of the protein was allowed to occur overnight inside the incubator, after which they were taken out and centrifuged, and the supernatant was discarded. The pellet containing the cells was dissolved in 1X PBS to reconstitute, and this mixture was again centrifuged. The pellet from the second round of centrifuge was dissolved in Buffer A (20 mM HEPES, 500 mM NaCl) and sonicated under high frequency in order to lyse the cell membranes and the cytosolic contents (Including our protein) could come out (Note: A Protease inhibitor PMSF was added to prevent degradation of protein from an external protease).

- Along with this, an empty PD10 column was washed thoroughly with SDS detergent, ethanol and MilliQ and then finally loaded with Ni 2+ -NTA beads with a micropipette (mouth of the tip cut) and a plunger (Our protein contains 6*His residues at its N-terminus, which acts as a ligand for Ni 2+ -NTA, is present in the column so that only our protein gets immobilized while the rest gets washed away).

- After incubation, the column was thoroughly washed with Buffer A (As our protein is dissolved in the same Buffer) for 5-7 times in a similar manner by using a plunger and a micropipette, following which the sonicated cellular lysate was centrifuged in an Oakridge flask (This was done so as to ensure the soluble protein got separated from the cellular debris) following which the supernatant was collected and subjected to Ni 2+ NTA affinity chromatography by incubating it within the already washed column.

- Then, using the micropipette and plunger, the flow-through containing non-specific proteins was collected and discarded during the washing.

  Protein Quantification and Storage

  After this, an elution buffer was prepared by dissolving Imidazole to the appropriate concentration within Buffer B (20 mM HEPES, 150 mM NaCl). An elution buffer acts as a chemical remover of our protein of interest from the stationary column by competing for chemical interaction with the same column (Ni 2+ NTA in this case) with the protein of interest. The imidazole ring is the central hydrocarbon ring within Histidine, which interacts with the column, and henceforth its only through a solution of excess Imidazole that these non- covalent bonds between the Column and our Protein is broken. These elutes are collected in a same falcon tube, giving a net volume of 2.5 ml in the end.

- Now, in order to measure the concentration of our protein, we took a diluted solution of this fraction in Buffer B and a Blank containing the same volume of Buffer B, and then we measured their Absorbance at 280 nm. Through this Absorbance, we calculate the concentration of the protein by using. Beer-Lambert's law:-

$$A = E * c * 1 \tag{2.1}$$

  where A = Absorbance(has no units, since its a ratio)
  E = Molar Extinction Coefficient($M^{-1}cm^{-1}$) L = Length of column (in cm)

- Now, to further concentrate this protein, it was Dialysed against the same concentration of Buffer B(Dialysis is a process through which excess salts and ions dissolved along with an

organic substance is removed through the process of Diffusion from a region of their higher concentration to a region of their lower concentration through a semi-permeable membrane through which only small salts and ions can pass through).
In our case, the Dialysis was done against 150 mM HBS(Buffer B) to get rid of the imidazole from the eluted fraction.

- Now, finally, our proteins final concentration was measured using the same aforementioned method, and then stored in 10 Nitrogen at -80 C.

So, finally, the concentration of ybbr-(titin-I27)x8-dockerin is $\sim 4\ \mu M$ in 25 mM Tris pH 7.5, 150 mM KCl, 5mM $CaCl_2$. The Coenzyme A is at 20 mM in coupling buffer 50mM Na_2PO_4, 50 mM NaCl, 10 mM EDTA at pH 7.2. Coh III is at $\sim 100\mu g/mL$ ybbr-Cohesin-III in 20 mM Hepes-NaOH buffer pH 7.5, 1 mM MgCl2. We have Sfp at 10 μM in 50 mM Hepes, 10 mM $CaCl_2$.

2.1.1 Functionalization of Protein

Pulling proteins with non-specific binding has many drawbacks. The efficiency of the events per cycle is very low ($< 1\%$), and with non-specific binding, we do not have much control over where the protein is getting pulled. So to tackle these issues and to increase the reproducibility *Functionalization of protein.* One of the robust method of functionalizing proteins for HS AFM is established by using dockerin/cohesin III complex [26]. The interaction of this ultrastable dockerin/cohesin III complex can withstand force up to 300 pN, which is higher than the unfolding forces of most protein domains. Below, I will explain the functionalization process in detail.

1. The cantilevers and Glass coverslips were cleaned with acetone for 10 minutes.

2. The coverslips were immersed in Piranha solution(3:1 of $H_2SO_4 : H_2O_2$) The Piranha Solution was washed off by sonicating the coverslips in Acetone, Methanol, and then Milli Q for 5 mins each. The surfaces were dried off with a dry flow of Argon.

3. The coverslips and the cantilevers were UV cleaned for 15 mins.

   Explanation: Piranha cleaning and UV-ozone cleaning cause the Oxidation of all the contaminants, and it also activate the glass surface to create Si-OH groups, which create an ideal surface for silanization using ATPES((3-Aminopropyl)triethoxysilane)

4. They were dipped in 5% APTES solution in Ethanol(pure). Explanation: In the Silanization reaction, the Si-OH group of APTES and Si-OH of the glass surface reacts to form Si-O-Si bonds in the presence of 99.9% Ethanol.

Figure 2.1: The reaction of APTES with oxidised glass surface..

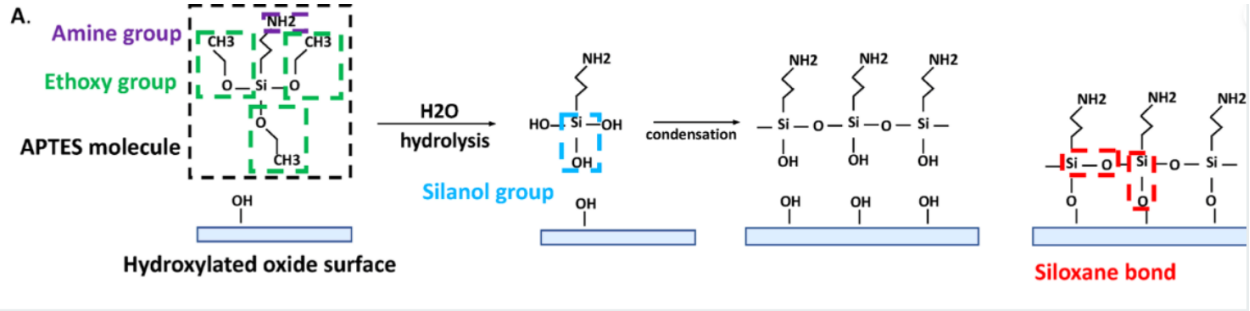

5. The Cantilevers and the coverslips are then rinsed properly with 99.9% Ethanol to wash off unattached APTES.

6. Then cantilevers and the coverslips are baked in the oven at 80°C for 1 hr. Immediately after this, they were immersed into Sodium Borate buffer in incubation at 4°C overnight. Explanation: Baking and keeping them overnight in alkaline conditions causes the deprotonation of the amine group of APTES which would later help in the attachment of other linkers.

   Day 2

7. They were rinsed 5 times with Milli Q.

8. They were incubated in 5mM of NHS-PEG-Maleimide for 1-2 hrs. Explanation: The NHS group in the linker would react with the amine group in APTES and the PEG-maleimide will attach to APTES via an ”-NH-” bond, which leaves out NHS in the process.

9. Rinsed again 5 times in MilliQ. And then incubated in 20mM of Coenzyme A dissolved in coupling buffer(50 mM Na_2PO_4, 50 mM NaCl, 10 mM EDTA pH 7.2) for 1 hour at room temperature. Explanation: This step ensures the attachment of Coenzyme A to the entire linker, via the;l ‘thiol-maleimide’ coupling reaction between the ‘SH’ group of Coenzyme A and the ‘NH’ group of maleimide via the Michael addition reaction.

10. Cantilevers and coverslips were rinsed 5 times in Milli Q and now they are ready for protein attachment.

11. **For Coverslips:** Incubated in varying concentrations of titin(from 8 μM to 30 μM), in reaction buffer 50 mM Hepes-NaOH, pH 7.5, 20 mM MgCl2 and 1mM CaCl2 in presence 1μM Sfp for 1 hour at room temperature for 2 hours.

    For Cantilevers: Incubated in varying concentrations of CohIII(from 8 μM to 30 μM), in reaction buffer 50 mM Hepes-NaOH, pH 7.5, 20 mM MgCl2 in presence 1μM Sfp for 1

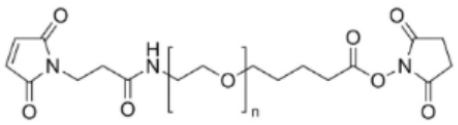

NHS-PEG-Maleimide

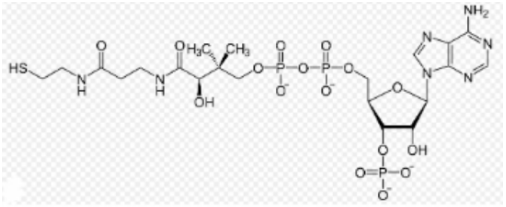

Coenzyme A

(a) NHS-PEG-Maleimide (b) Coenzyme A

Figure 2.2: Molecular structures of NHS-PEG-Maleimide and Coenzyme A

hour at room temperature for 2 hours. Explanation: Both the constructs of Titin and CohIII contain a ybbr sequence at their N-terminus. This sequence is a peptide that is specifically targeted by the Sfp1 enzyme for attachment with CoA-R(The 'R' in this case is the entire linker described so far). This reaction causes attachment of the functional group 'R' with the ybbr sequence along with the entire protein, leaving out CoA in the process. This is how Titin and CohIII get immobilized with the linker onto their respective surfaces.

12. After this the cantilevers and the coverslips were rinsed with PBS(pH 7.2) 5 times and then stored in PBS till the experiment.

2.2 Atomic Force Microscopy

Atomic Force Microscopy(AFM) is a type of scanning probe microscopy (SPM). In SPM,a sharp probe is used to interact with the sample, and a change in some parameters is utilized to extract the sample properties due to that interaction.

In AFM, a micro-cantilever is used as a probe. One end of the cantilever is fixed, and the other end has a tip that is made to interact with the sample(Fig.2.4). The interaction causes a deflection in the cantilever, which a detection scheme detects. When the deflection is small, the cantilever behaves like a Hookean spring. According to the application, the AFM is used in different modes. Static Mode: Also known as contact mode, the cantilever continuously stays in contact with the surface, dragging the tip along the path and taking the deflection of the cantilever to adjust the distance from the surface to maintain constant deflection.

Dynamic mode(dAFM): Also known as tapping mode, where the cantilever oscillates with a frequency and the interaction with the sample causes a change in amplitude, frequency and phase. According to the feedback parameter, there are two types of dAFMs, Amplitude modulation(AM dAFM) (where a change in amplitude is used for the feedback mechanism) and Frequency modulation(where a change in frequency is used for the feedback mechanism)

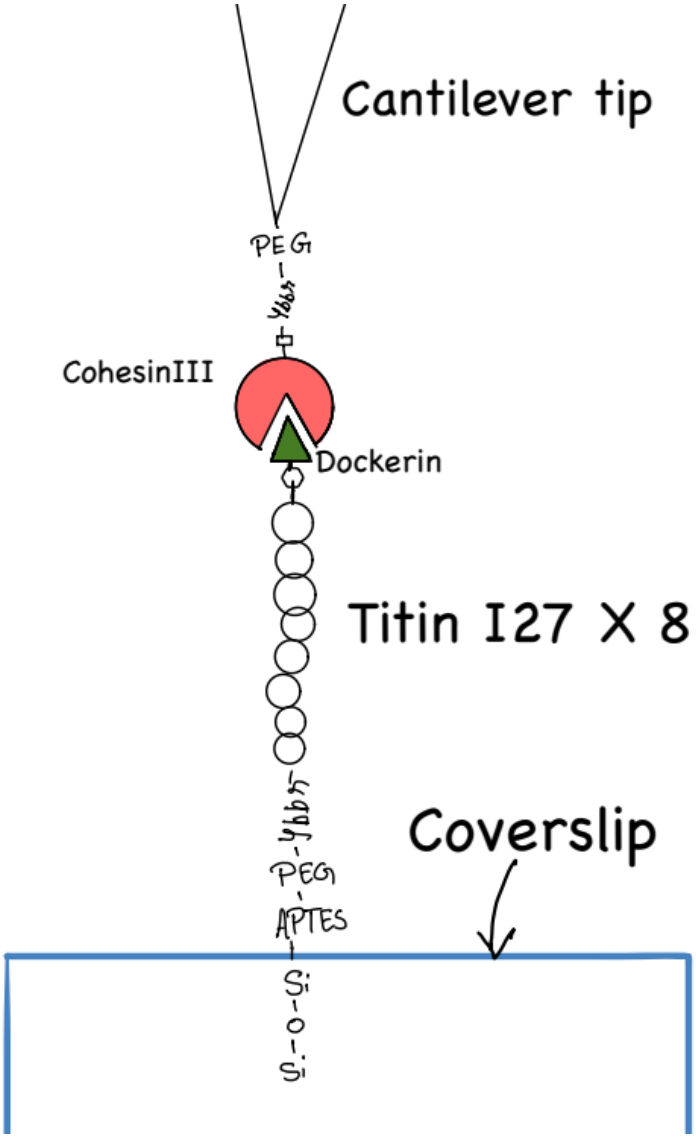

Figure 2.3: Schematic of Polyprotein ybbr-(titin-I27)x8-dockerin with ybbr tag at the N-terminus and dockerin at the C terminus. On Cantilever cohesin III is attached via maleimide and APTES. The cohesin III/dockerin bond formation is used for the specific pulling of the protein

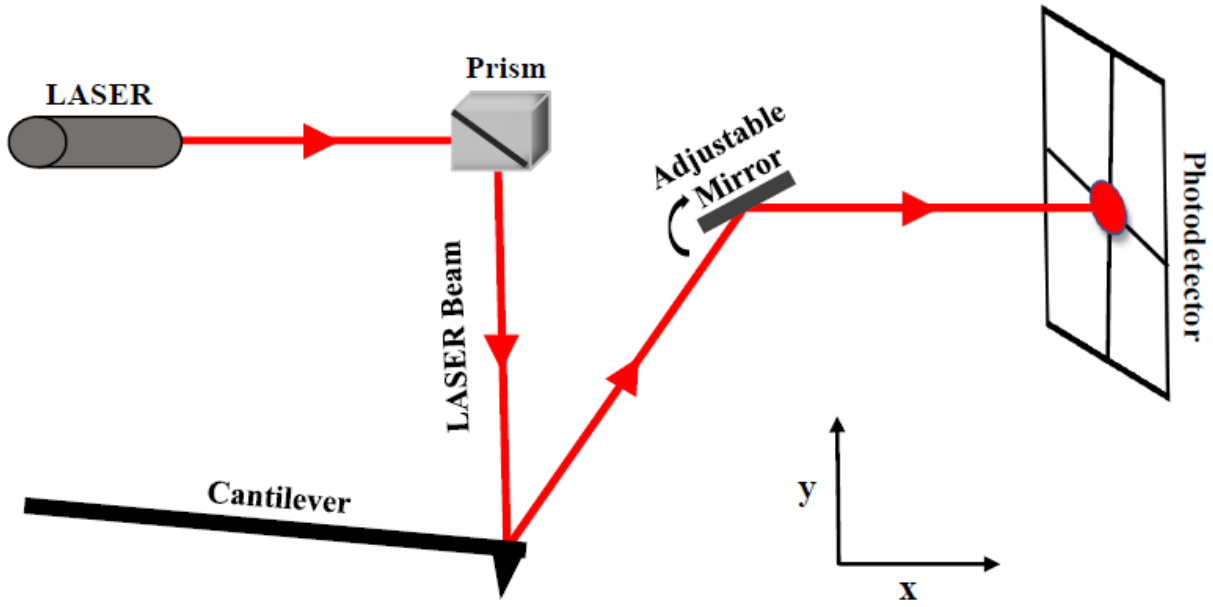

Figure 2.4: Schematic of AFM where laser is used to measure the cantilever deflection. When there is a small deflection in the cantilever, it causes the change in the laser position on the photodetector.

2.3 Commercial AFM

A commercial AFM has five major elements: detection system, cantilever tip assembly, cantilever/sample motion controller, feedback circuit and data acquisition. We have used *JPK Nanowizard II* for some calibrations and protein concentration optimization.

In commercial AFM, a laser is used to measure the deflection in the cantilever; this is known as *optical beam deflection detection method*. The laser is aligned on the back of the cantilever, as shown in Fig.2.4. With the help of an adjustable mirror, the beam is reflected on a four-quadrant position-sensing photodetector. The photodetector senses the vertical and horizontal motion of the cantilever. The photodetector's output voltage signal changes correspond to the cantilever's deflection. The optical sensitivity of the detection system is measured by taking a force curve on a hard surface. If the surface is clean and there is negligible indentation on the surface then the force curve (deflection in V vs base position) should be linear. The inverse of the slope of this linear fit will be the optical sensitivity. *Therman noise method* determines the force constant of the cantilever in the commercial AFM [13]. This method is based on the equipartition theorem. When the cantilever is in equilibrium with its surroundings, the average value of each quadratic term in Hamiltonian is given by:

$$\frac{1}{2}k_c < z^2 >= \frac{1}{2}k_B T \tag{2.2}$$

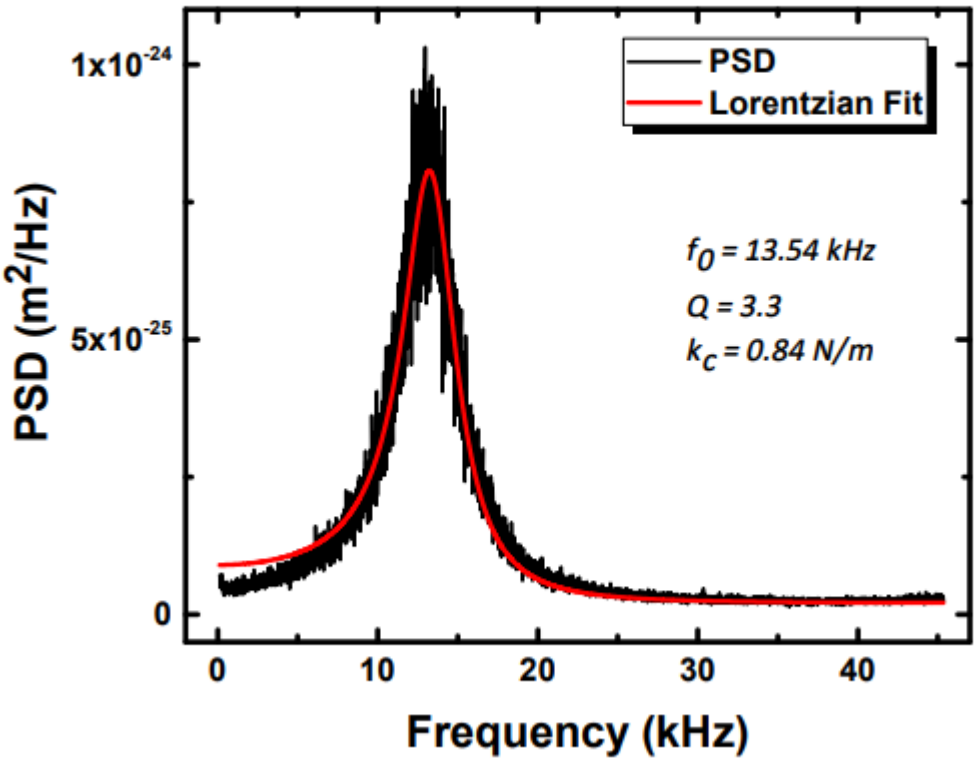

Figure 2.5: Caption

where K_B, T, k_c, $< z^2 >$ are Boltzmann constant, absolute temperature, force constant of the cantilever, and mean square displacement, respectively. Here $< z^2 >$ ($\sum < z_n^2 >$) (fig 2.5) is the sum of the mean square displacement corresponding to each eigenmode; this can be estimated by measuring the power spectral density (PSD). We can apply Lorentzian fit to the fundamental frequency mode by in-built functions, which will calculate the k_c.

2.4 Home built interferometer based AFM

Just like the commercial AFM, our Home-Built AFM also has five major parts 2.6:

1. Displacement detection system
2. The cantilever tip assembly
3. Cantilever and Sample motion controllers.
4. Feedback circuit

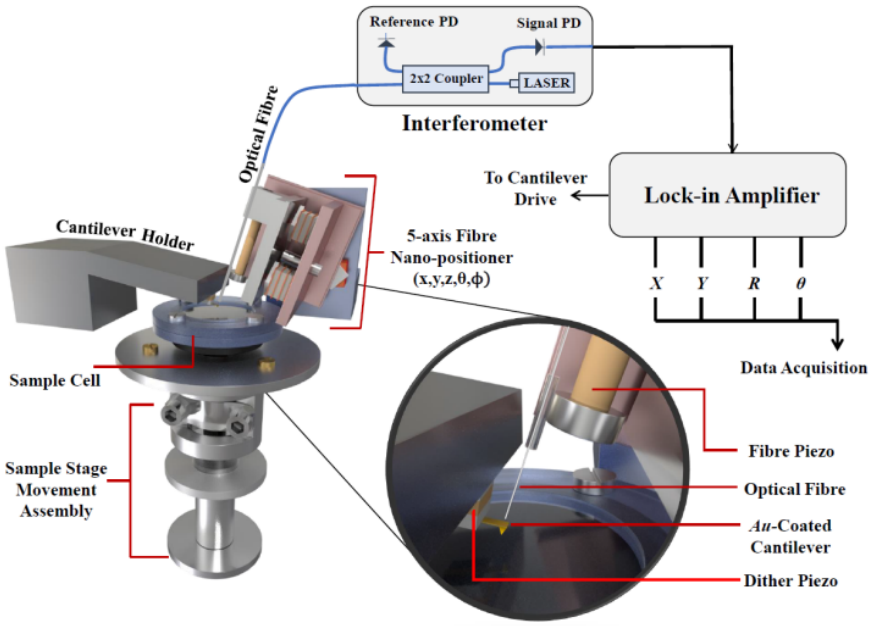

Figure 2.6: Schematic of home-built AFM.The magnified portion shows the alignment of the optical fibre parallel to the back surface of the cantilever.

5. Data acquisition and the display

The home-built AFM uses a displacement scheme instead of deflection detection. The advantages of using displacement detection are discussed in detail in later chapters.

2.4.1 Displacement detection system:

The alignment of the optical fibre on the cantilever's back surface is done with the help of inertial nanopositioners. This creates a Fabri-Perot cavity between the cantilever surface and the cantilever cross-section. The aligned end of the optical fibre acts as a partly reflective mirror. The partly reflective mirror is prepared by first cleaving one end of the $9\mu m$ diameter optical fibre with a high precision cleaver and then dipping in a metal-organic solution of *Titanium-(IV)-ethylhexoxide* and *p-xylene* with 1:2 weight ratio and then the end is flashed above a Butane torch. It makes the end of the optical fibre $\sim 25\%$ reflective. An infrared laser(λ =1310nm) other end of the fibre is passed through the fibre, which partly reflects back from the prepared end and partly transmits through; this transmitted part further gets reflected from the back surface of the cantilever and then again passing through the optical fibre. These two reflected beams(from the partially reflective mirror and the cantilever) interfere with each other, and the interference depends on the distance between the two reflective surfaces. The photo-diode detects the interfered laser, as shown in the figure. 2.7 The distance between the optical fibre and the cantilever is maintained constant at the point of maximum sensitivity (*Quadrature-point*). This arrangement gives the resolution of orders of Å.

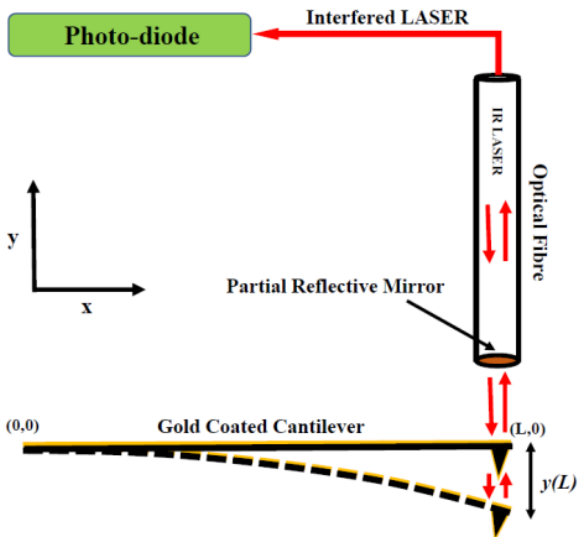

Figure 2.7: Figure shows partly reflective optical fibre aligned parallel to the back surface of a gold-coated cantilever which acts as a mirror. This arrangement creates a Fabri-Perot cavity, where the interfered laser is passed to a photo-detector, which converts the laser signal to a current signal as a function of the distance between the mirrors.

2.4.2 Nano-positioners

The alignment of the optical fibre is done using this nanopositioner assembly, which consists of two perpendicular plates, each held by magnets and there are three shear piezos arranged in such a way that they provide X, Y, Z, ϕ and ϕ motions when applied logical pulses.

2.4.3 Detection Sensitivity

The photo-diode output voltage per unit displacement of the cantilever. To determine the detection sensitivity after the parallel alignment of the optical fibre and cantilever, the optical fibre is oscillated by applying 100V amplitude sinusoidal voltage to the fibre piezo while the cantilever is kept stationary. The oscillating fibre generates an interference pattern at the photodiode. The system plots the output voltage vs the fibre motion and we can find the maximum slope using *find quadrature automatcally* and we can lock the position of the cantilever to the optical fibre(*quadrature point*).

2.4.4 Sample Stage Movement

The sample stage consists of three components: a platform for the sample cell, the hammer and the scanner piezo. The approach of the cantilever and the scanning is done by moving the sample cell, which is mounted on the sample stage and has stable magnetic contact. The Hammer piezo is used for the approach of the sample to the cantilever, and the Scanner piezo for the X, Y, and Z movements during the experiment [20].

2.4.5 Phase Sensitive Detection

Lock-in Amplifier SR830(Stanford, US) has been used for digital signal processing in Home-built AFM. The cantilever is excited using diether piezo from the Lock-in Amplifier's internal oscillations. The detector's output, containing the signal from the oscillating cantilever, is fed into the Lock-in Amplifier. The lock-in amplifier then isolates and measures the amplitude and phase of the cantilever's oscillation. The amplitude and the phase are the observables of our experiment and are further used to extract the properties of the sample. Phase-sensitive detection is a powerful method used to extract a signal even if it is buried in high noise[4]. As there are two parameters we need to extract, we need two phase-sensitive detectors(PSDs). The PSD1 multiplies the input signal and the reference signal and gives:

$$V_{PSD1} = V_r V_s Sin(f_s t - \phi_s) Sin(f_r t - \phi_r) \tag{2.3}$$

$$V_{PSD1} = \frac{V_r V_s}{2}[Cos((f_s - f_r)t + (\phi_s - \phi_r)) - [Cos((f_s + f_r)t + (\phi_s + \phi_r))] \tag{2.4}$$

The output of V_{PSD1} is passed through a low-pass filter which filters out the higher-frequency component $(f_s + f_r)$ and we are left with:

$$V_{PSD1} = \frac{V_r V_s}{2}[Cos((f_s - f_r)t + (\phi_s - \phi_r))] \tag{2.5}$$

In our case, we are using the internal oscillations of the lick-in amplifier to excite the cantilever and also for the reference signal so, $f_r = f_s$ then the equation 2.5 becomes:

$$V_{PSD1} = \frac{V_r V_s}{2}[Cos((\phi_s - \phi_r))] \tag{2.6}$$

$$V_{PSD1} \sim X = V_s Cos(\phi) \tag{2.7}$$

where $\phi = \phi_s - \phi_r$ is the phase lag between the reference and the signal.
To measure the Amplitude we use another PSD with reference signal phase shifted by 90°. Similar to V_{PSD1} the multiplied signal from V_{PSD2} is:

$$V_{PSD2} = V_r V_s Sin(f_s t - \phi_s) Sin(f_r t - \phi_r - 90^\circ) \tag{2.8}$$

Following the same steps as PSD1, we pass the signal of PSD2 through a low pass filter and we have $f_r = f_s$ V_{PSD2} becomes:

$$V_{PSD2} = \frac{V_r V_s}{2}[Cos((\phi_s - \phi_r - 90^\circ))] \tag{2.9}$$

$$V_{PSD2} \sim= Y = V_s Cos(\phi) \tag{2.10}$$

From the equations 2.7 and 2.10, we can calculate the Amplitude and the phase lag of the signal as:

$$A = \sqrt{X^2 + Y^2} \tag{2.11}$$

$$\phi = arctan\frac{Y}{X} \tag{2.12}$$

It is important to note that we did not consider the noise in V_s as the frequencies average out to zero.

2.5 Theory of Dynamic AFM

Introduction

There are two major modes in dynamic AFM: Amplitude modulation dAFM and frequency modulation dAFM. The feedback parameters of the two modes are different, AF-AFM uses amplitude as feedback parameter and FM AFM utilises both frequency and phase.
For viscoelastic materials, measurements of creep or relaxation are carried out for minutes or hours, which is impossible for cases such as proteins. Here, dynamic techniques such as dynamic AFM are used where sinusoidal stress is provided, and the response is measured.

$$\sigma(t) = \sigma_o sin(ft) \tag{2.13}$$

the stress-strain relation for elastic solids is:

$$\sigma = k\varepsilon \tag{2.14}$$

where , σ, ε, are the stress and the strain, and k is Young's modulus, the strain response will be:

$$\varepsilon(t) = \frac{\varepsilon_o}{k} sin(ft) \tag{2.15}$$

here the strain amplitude is $\frac{\sigma_o}{k}$ and the response is in phase with the stress. For viscous liquids,

$$\frac{d\varepsilon}{dt} = \frac{\sigma}{\eta} \tag{2.16}$$

where η is the coefficient of viscosity, the strain response will be:

$$\varepsilon(t) = \frac{\sigma_o}{\eta f} cos(ft) = \frac{\sigma_o}{\eta f} sin(ft - \frac{\pi}{2}) \tag{2.17}$$

the strain response lags behind by $\frac{\pi}{2}$ from the stress provided.

For viscoelastic materials, the phase laf will be ϕ where $0 < \phi < \frac{\pi}{2}$

$$\varepsilon(t) = \frac{\sigma_o}{\eta f} sin(ft - \phi) = \frac{\sigma_o}{\eta f}[sin(ft)cos(\phi) - cos(ft)sin(\phi)] \tag{2.18}$$

Hence, the response is a combination of both viscous and elastic responses. To separate these two, one needs to calculate the amplitude of the strain and phase lag with respect to the sinusoidal stress provided.

As a result, the response combines elastic and viscous responses. Calculating the strain amplitude and phase lag in relation to the given sinusoidal stress is necessary to distinguish between the two responses.

2.5.1 Point Mass Model

This simple yet useful model describes the dynamic of a cantilever with a spring attached to a point mass[21]. It describes the dynamic of the cantilever as a forced damped oscillator. The effective force constant of the cantilever is represented by the spring with spring constant k (fig.2.8). The equation of the damped oscillator can describe the motion of the cantilever as:

$$m\frac{d^2z(t)}{dt^2} + \gamma_c\frac{dz(t)}{dt} + k_c(z - z_o) = F_i \tag{2.19}$$

where m = 0.25 m_c is the effective mass of the point mass corresponding to the cantilever and cantilever m_c, γ the cantilever's real mass, and its damping coefficient z is the displacement of the cantilever from its equilibrium position z_0 and F_i is the external force on cantilever due to interaction. This paper checks the validity of the point mass model.[21]

2.5.2 Exciatation mode

As shown in figure 2.8 one can use the two excitation schemes for dynamic force spectroscopy experiments. The point mass model's essential assumption is that the cantilever's frequency response is far from its fundamental mode. The cantilever's resonance frequency from this mode is f_0, k_c being the cantilever spring constant and γ_c being the damping coefficient. These parameters are calculated by fitting a Lorentzian to the power spectral density(2.5) in commercial AFM.

Base Excitation: As shown in fig2.8(a), the cantilever's base is excited sinusoidally with Ae^{ift}. The cantilever is modelled with a point mass model, with spring constant k_c moving in a surrounding medium with damping coefficient γ_c. Due to the attached sample, the cantilever feels some interaction force F_i. The force equation of the point mass can be obtained by modifying the

equation 2.19 as:

$$m\frac{d^2z(t)}{dt^2}+\gamma_c\frac{dz(t)}{dt}+k_c(z(t)-Ae^{ift})=F_i \tag{2.20}$$

$$F_i=\bar{k}z(t)+\bar{\gamma}\frac{dz(t)}{dt} \tag{2.21}$$

m: effective cantilever mass and z is the deflection in the cantilever. For linear viscoelastic material, we can assume the Kelvin-Voigt model; then we can write the interaction force as $F_i = \bar{k}z(t)+\bar{\gamma}\frac{dz(t)}{dt}$. Here $\bar{k}$ and $\bar{\gamma}$ are the stiffness coefficient and friction coefficient, respectively. Putting the value of F_i we can write the equation 2.20 as:

$$m\ddot{z}+(k_c+\bar{k})z+(\bar{\gamma}+\gamma_c)\dot{z}=k_cA_0exp(ift) \tag{2.22}$$

2.5.3 Tip Exciatation:

Similarly, for fig2.8(b) when the tip is directly oscillated with force F_0e^{ift} the equation of motion for cantilever (b) can be written as:

$$m\frac{d^2z(t)}{dt^2}+\gamma_c\frac{dz(t)}{dt}+k_cz(t)-F_0e^{ift}=F_i \tag{2.23}$$

$$m\ddot{z}+(k_c+\bar{k})z+(\bar{\gamma}+\gamma_c)\dot{z}=k_cA_0exp(ift) \tag{2.24}$$

Here, A_0 is tip's amplitude due to the applied force F_0 Both 2.23 and 2.24 are the equations of forced damped oscillators and can be solved for the values of $\bar{k}$ and $\bar{\gamma}$.

2.5.4 Near Resonance Measurements

For both tip excitation and base excitation the cases the equations can be solved as forced-damped oscillators. The solution of the forced damped oscillator is well known as:

$$|A|=\frac{k_cA_0}{\sqrt{(k_c+\bar{k})^2\left(1-\frac{f^2}{f_0^2}\right)^2+(\gamma f)^2}} \tag{2.25}$$

$$tan\phi=-\frac{\gamma f}{(k_c+\bar{k})\left(1-\frac{f^2}{f_0^2}\right)} \tag{2.26}$$

where $f_0 = \sqrt{\frac{k_c+\bar{k}}{m}}$ and $\gamma=\bar{\gamma}+\gamma_c$

So, in theory, if we accurately measure the A and the ϕ due to the interaction as the oscillated frequency, we can calculate the $\bar{k}$ and $\bar{\gamma}$. However, measuring the amplitude and the phase response

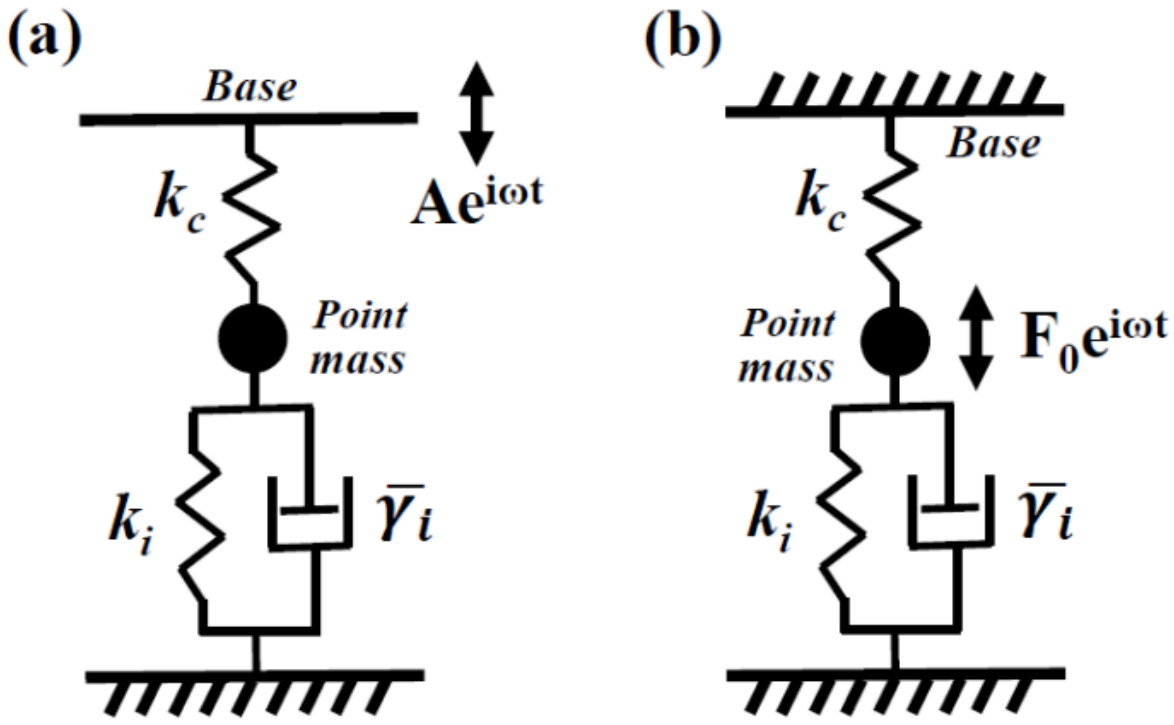

Figure 2.8: Schemetic of the point-mass model in two different modes of excitations. The force constant of the cantilever is represented by the spring constant k_c and the interaction of the sample is represented by a spring k_i and damper γ_i in parallel (Kelvin–Voigt model) (a) Base excitation with Ae^{ift} and (b) Tip excitation with F_0e^{ift} with help of magnetic excitation or other methods.

without any artefact has always been very challenging. When the measurements are done on or near resonance, it is very difficult to characterise the cantilever's dynamic. The dynamic of the cantilever itself dominates the pN and nm scale interaction of the protein interaction. Also, it is very difficult to control the amplitude and predict the phase behaviour of the cantilever[19, 14, 31]. One of the solutions to this problem is directly exciting the tip by magnetic[11] or photo-thermal [28] methods. Because of these issues, it is suggested that dynamic force spectroscopy experiments be performed on an off-resonance regime. In the later section, we will discuss the advantages of the off-resonance regime.

2.5.5 Off-Resonance Measurements

When working at a frequency much far below the resonance frequency of the cantilever ($\omega << \omega_0$) the term $\left(1-\frac{f^2}{f_0^2}\right)^2$ in equation 2.25 and 2.26 becomes 1 also, the damping coefficient of the cantilever γ_c is much less than that of the friction coefficient of the interaction $\bar{\gamma}$. Hence $\gamma = \bar{\gamma}$. And the equations 2.25 and 2.26 becomes :

$$|A| = \frac{k_c A_0}{\sqrt{(k_c+\bar{k})^2 + (\bar{\gamma}f)^2}} \tag{2.27}$$

$$tan\phi = -\frac{\bar{\gamma}f}{(k_c+\bar{k})} \tag{2.28}$$

Equation 2.28 can be becomes:

$$(k_c+\bar{k}) = -\frac{\bar{\gamma}f}{tan\phi} \tag{2.29}$$

We can substitute this equation in equation 2.27, and we have:

$$|A| = \frac{k_c A_0}{\sqrt{(-\frac{\bar{\gamma}f}{tan\phi})^2 + (\bar{\gamma}f)^2}} \tag{2.30}$$

By solving this equation, we get the:

$$\bar{\gamma} == \frac{k_c A_0}{|A|f} Sin\phi \tag{2.31}$$

And

$$\bar{k} = k_c\left(\frac{A_0}{|A|}Cos\phi - 1\right) \tag{2.32}$$

Off-resonance measurements primarily aim to drive the cantilever at a low enough frequency to cause very little inertial force and damping, allowing the cantilever to be modeled as a static system.

If the cantilever has no sample attached, then $F \approx (A–A_0)k_c$ where $(A–A_0)$ is the deflection. Also, $\phi \approx 0$ means no phase lag between the drive and the response.

2.5.6 Displacement detection scheme

As discussed earlier, there can be phase lag due to hydraulic damping while working with a cantilever oscillated near resonance. It will also be difficult to control the amplitude near resonance. Interacting with the sample can increase the cantilever's resonance frequency, reducing its amplitude and the phase lag. This decrease in phase lag due to the resonance frequency change can cause misinterpretation. So, it is better to reduce the phase lag due to hydrodynamic drag as much as possible.

To satisfy the condition of true off-resonance, cantilevers with higher stiffness and good quality factors are recommended. Figure 3.4 shows two cantilevers' amplitude and phase plots (point mass model). The left curves are for a cantilever with low stiffness and quality factor, and the right two for a cantilever with higher stiffness and quality factor. Suppose we are working at a frequency of 350 Hz (shown by a dotted line); when an additional interaction stiffness is attached to the cantilevers(a and c), there is a significant change in the phase lag in the case of the cantilever with lower stiffness. However, the stiffer cantilever had negligible phase lag even before the interaction stiffness was attached. Later, there is negligible change in the phase lag due to the extra stiffness. Also, a small amplitude is recommended to maintain the material's linear response. So, considering all these issues, the cantilever has a higher stiffness of 0.6-1 N/m and a high resonance frequency in the water of 25-50 KHz, which is used in interferometer-based AFM measurements. This allows us to reach a true off-resonance regime where the phase lag is negligible due to hydrodynamic damping, and the only phase lag that will be observed will be due to the interaction with the sample. The amplitude is kept around 1 nm to maintain the linear response. However, the drawback of using a stiffer cantilever is that they also have lower force sensitivity. The change in amplitude will be much less due to the interaction. Hence, they will have a low signal-to-noise ratio, which is impossible to measure using the conventional deflection detection scheme(fig 2.9).
As I mentioned earlier, the home-built AFM uses an interferometer-based technique to measure the displacement of the cantilever. This displacement detection scheme has a great advantage over the conventional deflection detection used in the commercial AFM when working off-resonance.

Experiments on Home built:

After the purification of the protein, we had to decide the working concentration of the protein. For this purpose, we performed Non-oscillatory pulling experiments on Commercial JPK AFM. After optimization of the concentration, we decided to continue the experiments on the working concentration of 25 μ of titin I27-dockerin and 27μCohesin.
At this concentration, we got $> 20\%$ of the curves with 5 or more unfolding events, which is

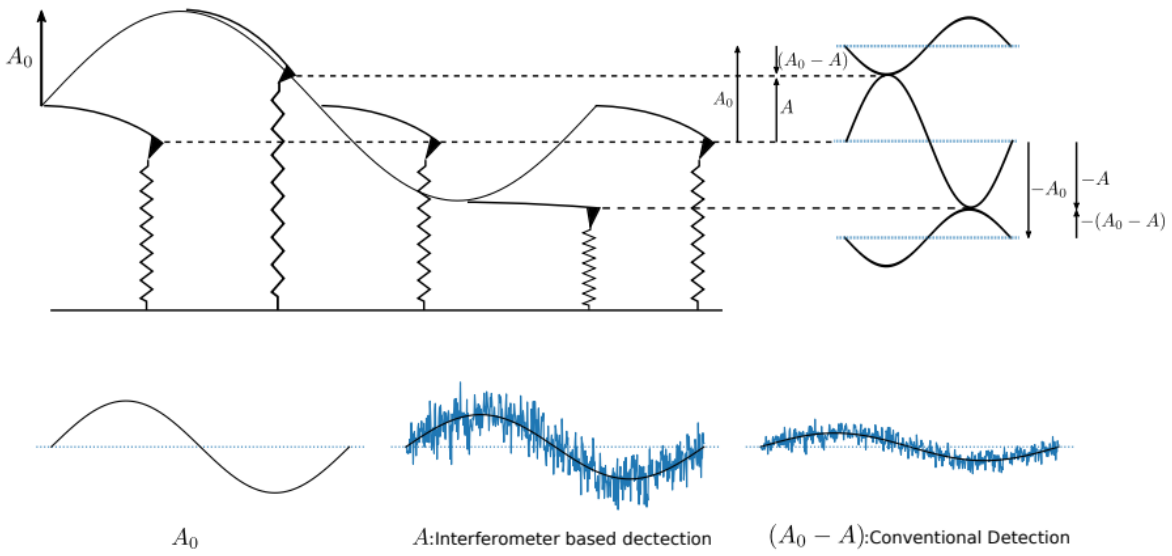

Figure 2.9: The difference between the conventional detection($A_0 - A$) and displacement detection. The cantilever is excited by the base with amplitude A_0, and the tip has amplitude A; the conventional detection measures $A_0 - A$ which has a much lower signal-to-noise ratio than the displacement detection, which measures A directly.

significantly higher than that of non-specific binding($\sim 1 - 2\%$).

One of the issues I faced during the experimentations on home-built AFM is I used Aluminium backside coated cantilevers (k=0.6 N/m) HQ:NSC36/Au BS With f_0 = 65kHz. Initially, we used aluminium backside-coated cantilevers. Still, during the experiments, we realised that the Aluminium coating of the cantilever is reacting with the PBS buffer and leads to the formation of H_2 bubbles on the cantilevers, which removes the Al coating and reduces the sum signal of the AFM. We tried coating the cantilevers with 4 nm Cr and 45 nm Au from the back side to resolve this. However, that also did not work as the coating got scratched during the functionalization and experiment. Finally, we used backside-coated cantilevers and functionalized them and they worked properly on the Commercial AFM.

As discussed earlier in this chapter, the inertial nanopositioners are used to align the optical fibre parallel to the back surface of the Cantilever. Although this alignment is done in the air Before performing any experiment in the home-built interferometer-based AFM, we have to align the . This alignment is done in the air. However, after functionalization, our cantilever is coated with cohesin protein which is to be kept wet. Otherwise, the protein will denature. We had difficulty aligning it fast enough so that the proteins in the cantilever didn't dry. The fastest alignment we could do was 4-6 mins, which is long enough for the protein to get destroyed.

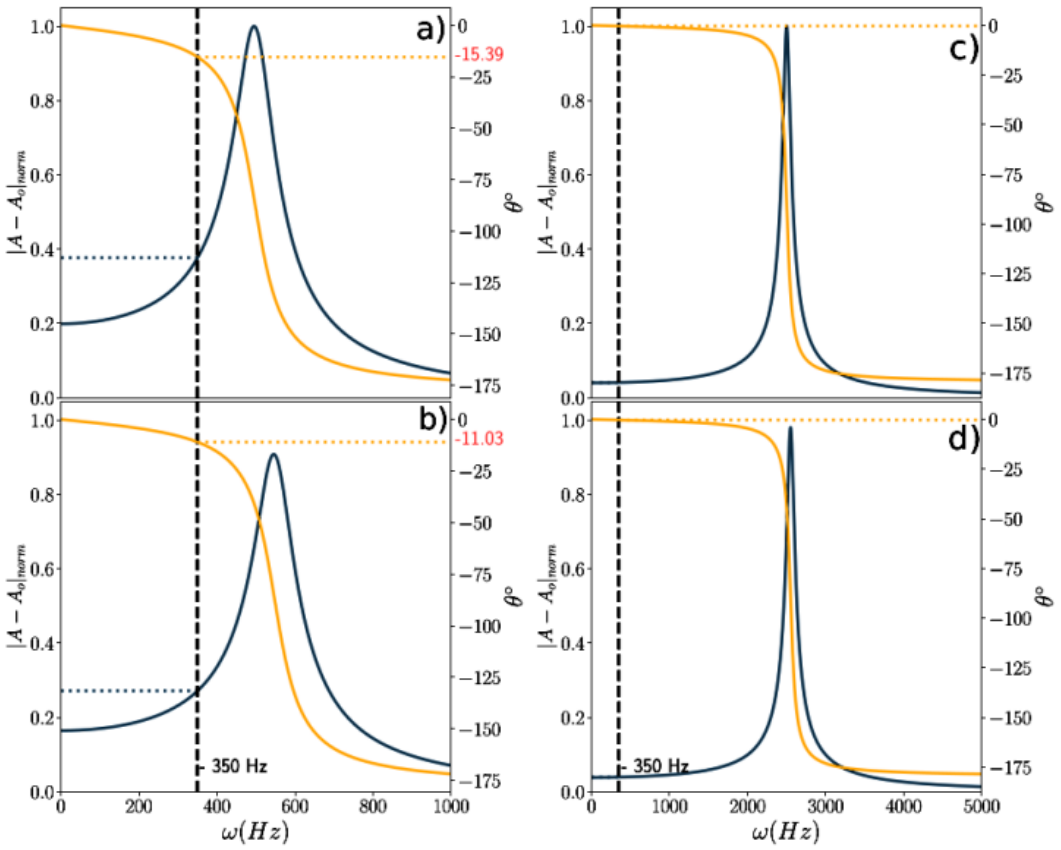

Figure 2.10: Plots of the solution of forced damped oscillator(Point mass model). a.)Phase and amplitude response of cantilever with low stiffness and quality factor b) same cantilever as a) but extra stiffness interaction is added to the cantilever stiffness. c) Cantilever with high stiffness and quality factor d) same as c) with extra stiffness interaction is added to the cantilever stiffness.

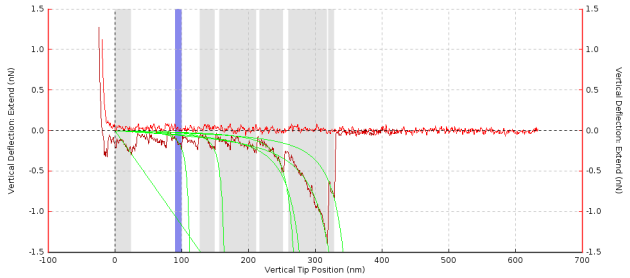

(a) Non-oscillatory pulling of the proteins on commercial AFM for optimization .

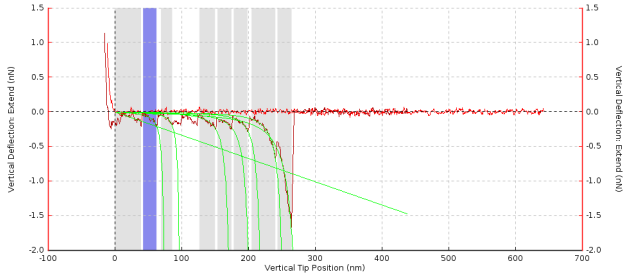

(b) Non-oscillatory pulling of the proteins on commercial AFM for optimization

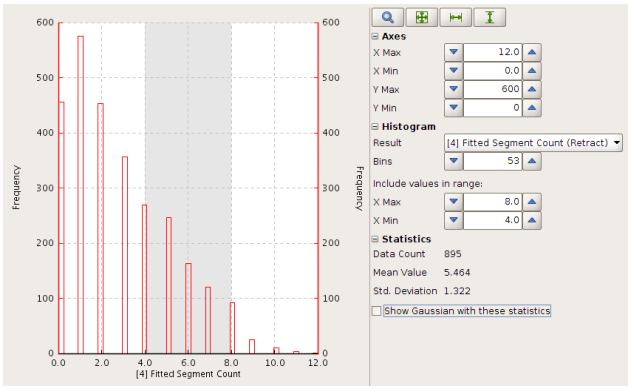

(c) Around 900 out of 2800 curves have ¿ 4 unfolding events at the optimized concentration.

Figure 2.11: Setup of High-speed AFM

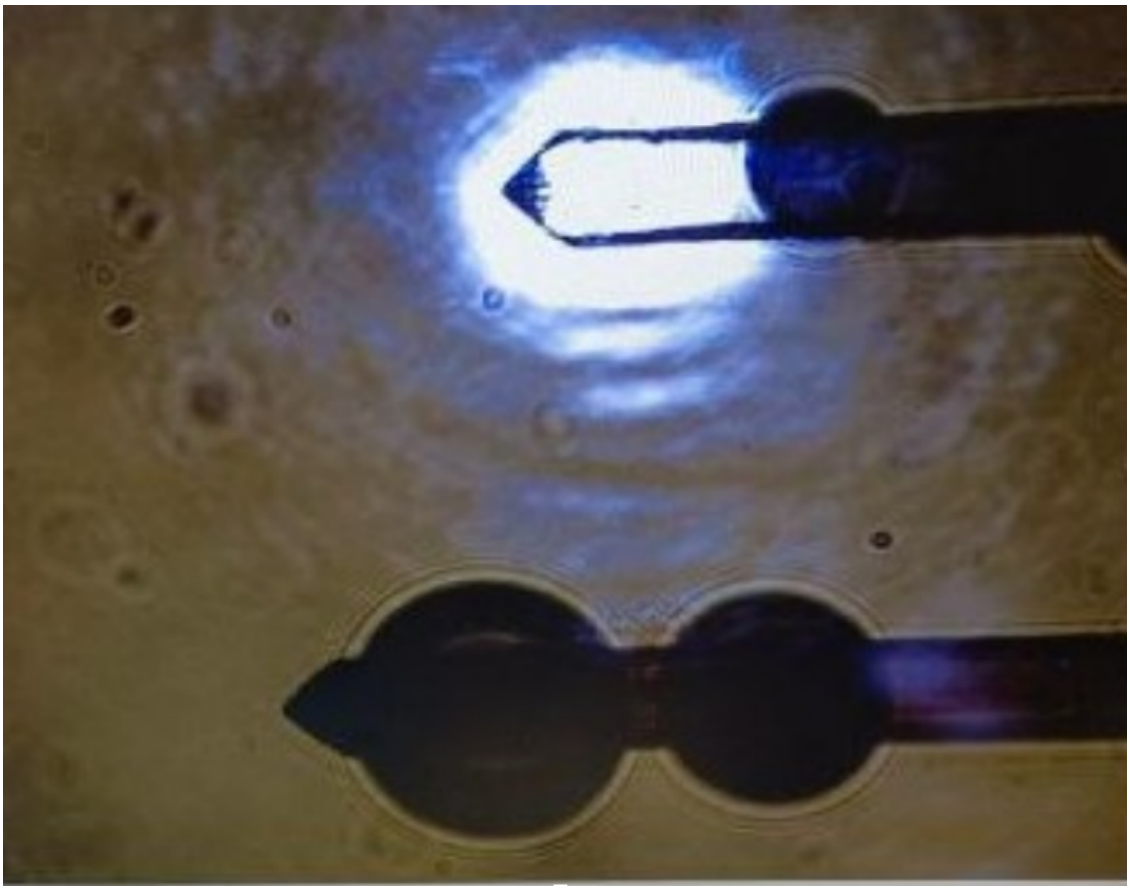

Figure 2.12: The Aluminium of backside coated Al cantilevers reacts with the PBS buffer and leads .to the formation of H_2 bubbles on the cantilevers, which removes all coating from the experiment

To continue with the same functionalization method, we would have to reduce the alignment time essentially.
To resolve the issue of fibre alignment, along with other issues, my lab colleagues have been working to redesign some aspects of the home-built AFM. With the new design, we will not have to realign the optical fibre every time we change the sample or the cantilever. In this new design (by Hrishikesh Ingole), the relative orientation of the optical fibre holder and the cantilever holder is kept fixed and minute adjustments can be made using the nanopositioners.
Once we set this new design, we will hopefully be able to do the alignment quick enough.

2.6 High Speed AFM

Since its invention in 1986, continuous developments have been made to improve the AFM and use it for many applications. It was initially used to probe hard surfaces in the air. In later developments, it was adapted for use in biological materials. There have been continuous attempts to make it much faster. Although it could capture biological samples' mechanical properties and image their topography, the imaging rates were always significantly slower than most biological processes scientists wanted to capture. The scanning rate was majorly limited by the sampling rate, which, in turn, depended on the cantilever's resonance frequency. The cantilever's geometry and dimensions decide the cantilever's resonance frequency. For rectangular cantilever the relation of the resonant frequency and its dimension is:

$$f_0 = \frac{1}{2\pi}\sqrt{\frac{k}{m}} \tag{2.33}$$

Where k, m is the spring constant and mass of the cantilever, t, w, L are the cantilever's thickness, width and length, and E is the Young's modulus of the cantilever material. With the technological advancement over time, the small enough cantilevers (2 x 6 μ m) were made. In 2001, Ando et al. [1] introduced the first High-speed AFM. The resonance frequency of this cantilever was $\sim$ 1 MHz underwater, so the Experiment could be performed at a much higher scanning rate. They could capture live biological processes at work with much faster feedback control and nm accuracy. With this high-speed AFM, they could capture the walking of myosin on actin at video-speed imaging rates. Before this walking of myosin was just theorized, capturing such processes gives much depth of these processes. The small size of the cantilever provides the capability of using it at the order of magnitudes faster(up to mm/s) than the speeds that could be reached by conventional AFM($\sim 10\mu m$) also, we could reach frequency 100s of KHz.

For High-Speed force spectroscopy High cantilevers AC10DS, Olympus and BL-AC40TS are used. The resonating frequency of the AC10 and AC40 cantilevers underwater is 400 kHz and 25

kHz, with spring constants 0.09 and 0.1, respectively. The dimensions of the AC10DS cantilever are 9x2x0.13 μm. The dimensions of the BL-AC40TS cantilever are 38×16×0.2 μm.

For my experiment, I used *RIBM SS-NEX* 2.13

Experimental procedure for HS AFM. I usually 4-5 1mm diameter glass coverslips and a few cantilevers for the HS AFM. I clean the surfaces and the cantilevers and did the functionalization as discussed in section 2.1.1. After the functionalization, the surfaces and the cantilevers are kept in PBS(pH 7.2) until the experiment is performed. Using the surfaces and cantilevers within 1-2 days is suggested for best results.

1. After washing with alconox and milli Q thoroughly, the cantilever cell (fig 2.13c) is filled with 150 μl of reaction experiment buffer(PBS).

2. Then the cantilever is screwed into the cantilever holder. This is then fixed on the top of the inverted microscope. It gets held in its position with the help of magnets in the cantilever holder and the stage below.

3. For the sample surface attachment with the sample stage (scanner), vacuum grease is used. With the help of thin copper wire, very little grease is applied on the sample stage. The 1 mm diameter coverslip is then rubbed dry with kimwipes tissue, quickly placed, and bit pressed on the greace applied earlier. With no time delay, a 3 μl drop is drop cast on the coverslip to prevent it from drying.

4. After alignment of the laser on the back of the cantilever, the scanner is placed on top of the cantilever cell as shown in fig 2.13a.

5. The cantilever calibration is done using the one-step calibration method[25], which is coded in a MATLAB program.

6. Once the approach is made and we start taking force curves, the cantilever is oscillated by applying a sinusoidal voltage signal to the cantilever using the external wave generator Agilent 33500B.

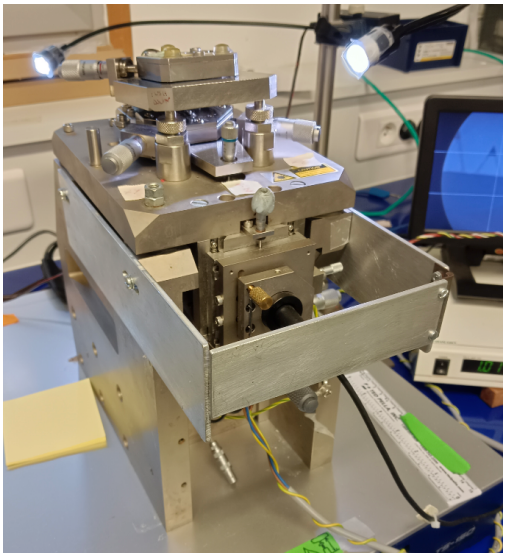

(a) HS-AFM with sample stage and cantilever cell mounted .

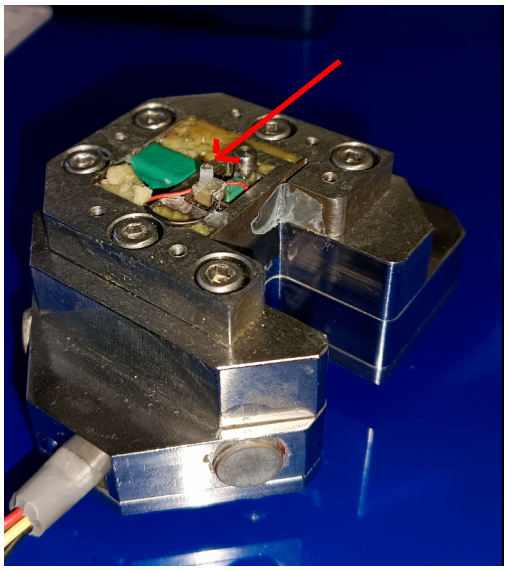

(b) Sample stage

(c) Cantilever cell.

Figure 2.13: Setup of High-speed AFM

Part II

Discussion and Conclusions

3

Discussion

3.1 Experimentation of High-Speed AFM AFM

We used Olympus AC40-TC-C2 and Olympus BL-AC10DS-A2 cantilevers for the high-frequency force spectroscopy experiments. The AC40 cantilever has a spring constant (k) = 0.09N/m and resonance frequency $\sim$ 25 kHz in water, it has dimensions 38×16×0.2 μm. The AC10 cantilever has a spring constant (k) = 0.1N/m and resonance frequency $>$ 100 kHz in water, it has dimensions 9×2×0.13 μm. These cantilevers are suitable for our aim to go to higher frequencies and still maintain the off-resonance regime.

With AC10 cantilever, we did experiments of frequencies up to 5 kHz and with AC10 we did experiments of frequencies 50kHz and 100 kHz.

As discussed earlier, the HS AFM uses deflection detection, which has a much lower sensitivity than displacement detection in the interferometer-based AFM.

3.2 Data Analysis

As discussed earlier (sec 2.4), the interferometer-based AFM uses displacement detection, unlike the deflection detection in HS AFM. With phase-sensitive detection and a lock-in amplifier, we directly get Amplitude(A) and Phase(ϕ) changes of the given oscillations as experimental parameters in the case of interferometer-based AFM. We can then solve the equations 2.31 and 2.32 to get $\bar{k}$ and $\bar{\gamma}$. On the other hand, we use deflection detection, so to use the same method to calculate

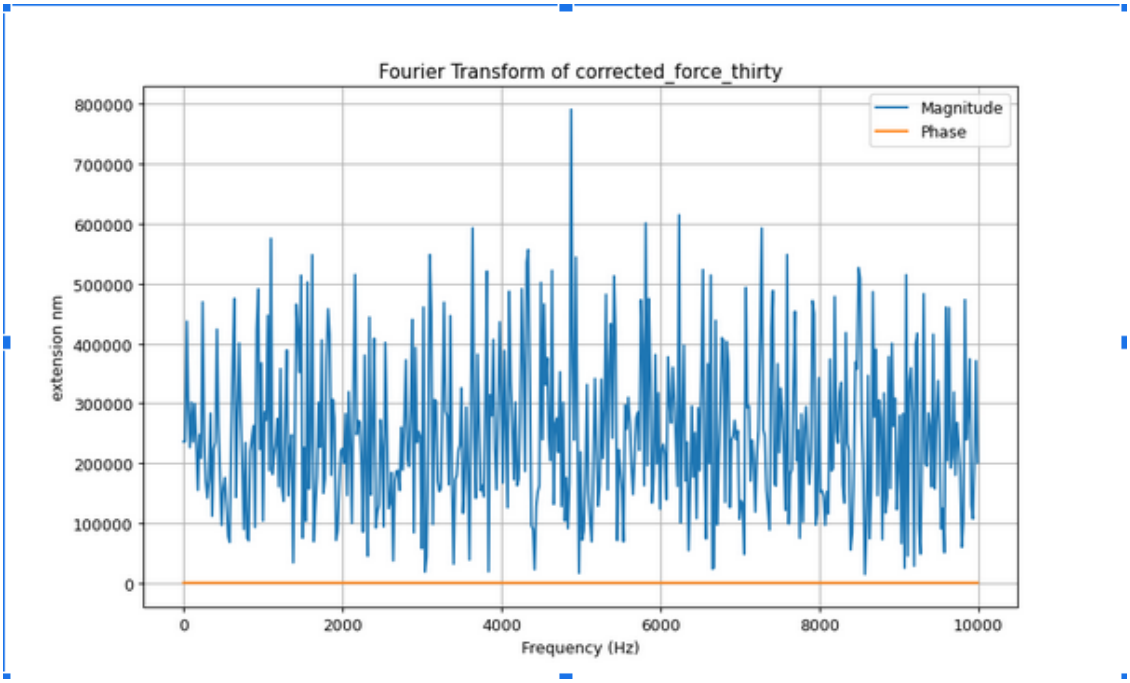

Figure 3.1: Caption

$\bar{k}$ and $\bar{\gamma}$, we have to extract Amplitude(A) and Phase(ϕ) changes from this data.

First, I converted the deflection signal into Force vs time data with the help of existing Python code. I Fourier transformed the data from the time domain (**??**) to the frequency domain (fig. 3.1). In the figure 3.1, the measurements are done at 5 kHz, as we can see the peak at that exact frequency. Other than that peak, everything else is noise. The signal-to-noise ratio is less. So, we can get the amplitude data from Fourier and transform the deflection data. However, getting the phase change from the deflection data is hard. Without the A and ϕ, we can not calculate $\bar{k}$ and $\bar{\gamma}$. Also, the Fourier transformation is for all data of a single force curve, so we do not get any event-specific details from the Fourier-transformed data.

So, the same method to calculate the $\bar{k}$ and $\bar{\gamma}$ can not be applied to the deflection data we got from HS AFM; hence, we had to consider other possible methods to calculate the viscoelasticity from deflection data.

One of the ideas we got from the work done by Rigato et al. [23]. In this work, they studied the microrheology of cells and calculated the complex shear modulus G*.

In this work, the cells are indented at several different frequencies, and the G* is calculated for all of them.

When a pyramidal cantilever tip is intended into a surface such as a cell, the Force-indentation relation is given by:

$$F = \frac{3Etan\phi}{4(1-v^2)}\delta^2 \tag{3.1}$$

where E is the elastic modulus, $\delta = z* - zc - d$ is the indentation, and v is the Poisson's ratio. The shear modulus and Elastic modulus are related to the equation:

$$G = \frac{E(1-v)}{2} \tag{3.2}$$

We can substitute equation 3.2 into 3.1, and we can Fourier transform the whole to go into the frequency domain and we get:

$$G* = \frac{(F-F_0)(1-v)}{3\delta tan\phi(\delta-\delta_0)} \tag{3.3}$$

Here $F(\omega)$ and $\delta(\omega)$ are now in the frequency domain.

$$G* \propto \frac{F(\omega)}{\delta(\omega)} \tag{3.4}$$

Where

$$G* = G_1 + iG_2 \tag{3.5}$$

Here G_1 and G_2 are Shear storage and shear loss moduli. G* represents the viscoelasticity property of a material.

In equation 3.3 the $\frac{(1-v)}{3tan\phi}$ depends on the geometry of the cantilever. So So if we calculate the force in the frequency domain and find its ratio to the extension in the frequency domain(which is indentation in the case of cells) it will be equivalent to some K*

$$K* = K1 + iK2 \propto \frac{F(\omega)}{\delta(\omega)} \tag{3.6}$$

Where K1 and K2 will be some elastic and viscous modulus. We would have to find the exact equation relating to these terms.

So, we can not directly measure the amplitude and the phase change due to the interaction. We convert the F(t) into frequency domain F(ω).

I am taking the raw force curve files and converting the force from the time domain to the frequency domain to somewhat relate the ratio of F(ω)/$\delta\omega$ to some K*

Where K* might be some complex elastic modulus.

Till now I have collected Data using two cantilevers AC10 and AC40 at frequencies 5kHZ, 10kHZ, 50kHZ and 100kHZ.

I will follow the same idea and try to draw some conclusions from the pattern we see in the

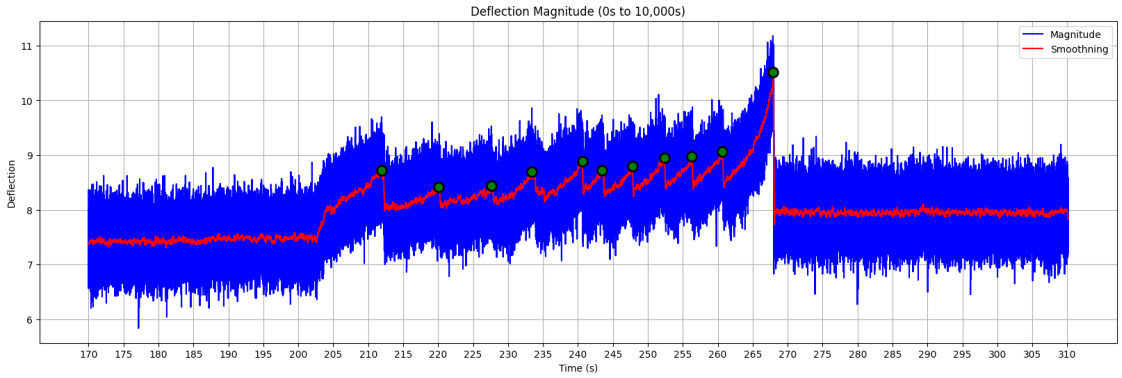

Figure 3.2: Plots Deflection in nm with soothed using savitzky window length = 1001, and peak detected

unfolding events of force curves.

After correcting the force and calculating the extension by data analysis, I Fourier transformed the force and the extension in Windows of 5 ms. I plot the K* comparing it with force as in Fig. 3.3

3.3 Conclusion

From the experiments done on the Interferometer based AFM, the direct values of force constant k and internal friction γ can be measured and have been in past study [8]. Viscoelasticity can also be estimated using the concept of Complex shear modulus, such as done in [23] on cells. We will further analyse our data for different frequencies and estimate these values.

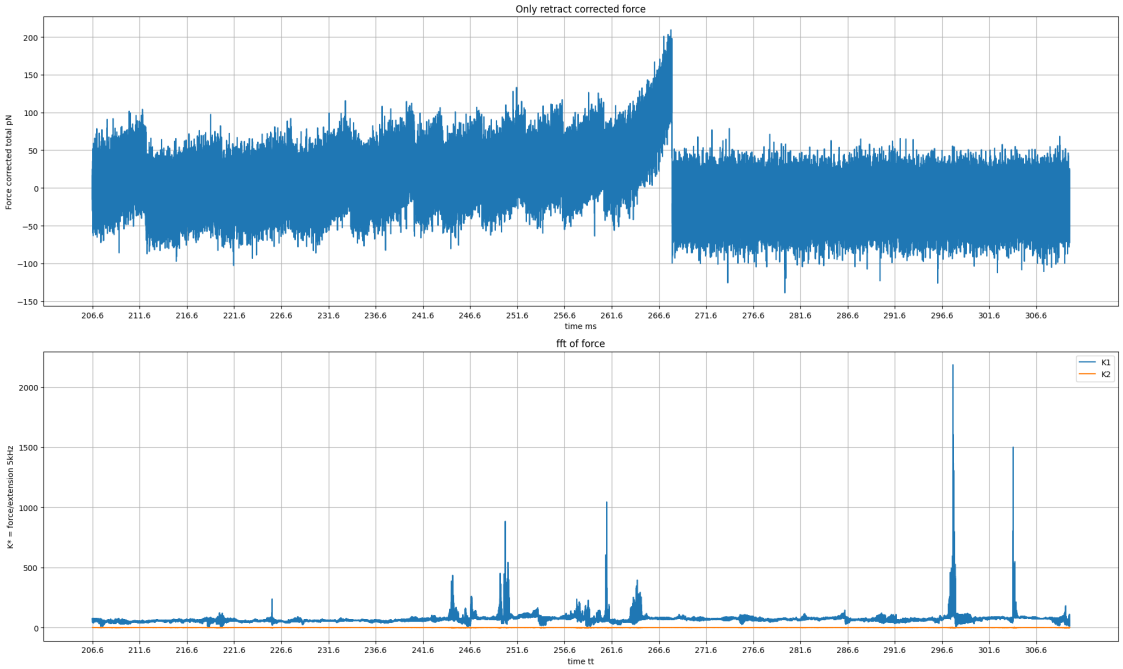

Figure 3.3: Force as compared to Complex K.

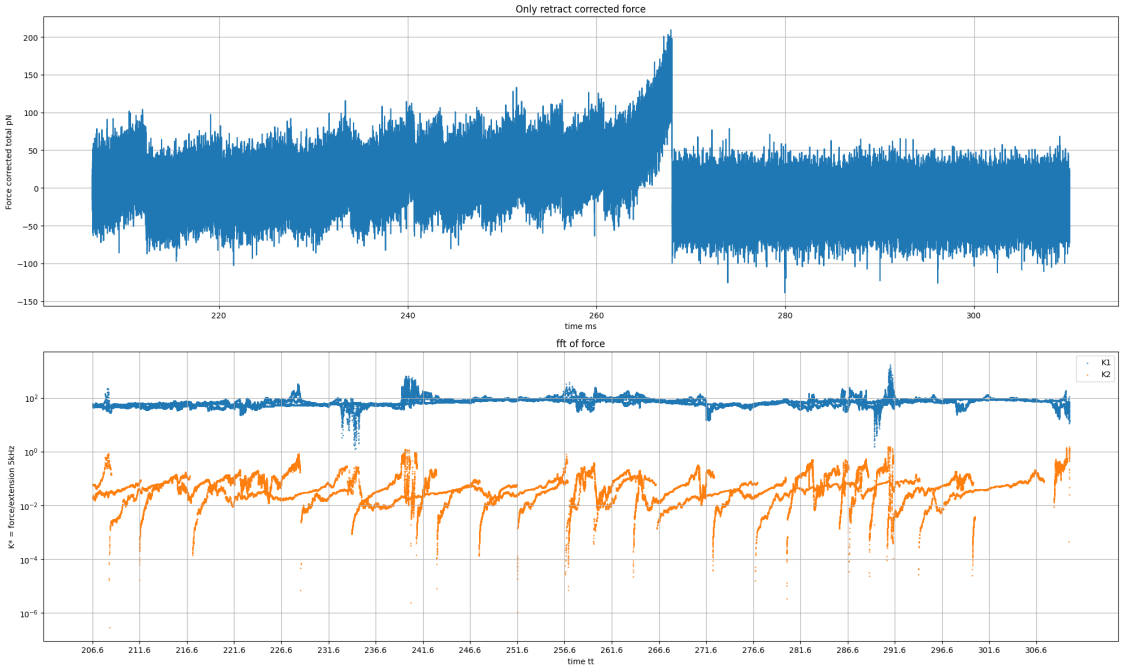

Figure 3.4: Force as compared to Complex K in logarithmic scale.

Bibliography

[1] Toshio Ando, Noriyuki Kodera, Eisuke Takai, Daisuke Maruyama, Kiwamu Saito, and Akitoshi Toda. A high-speed atomic force microscope for studying biological macromolecules. *Proceedings of the National Academy of Sciences*, 98(22):12468–12472, 2001.

[2] George I Bell. Models for the specific adhesion of cells to cells: a theoretical framework for adhesion mediated by reversible bonds between cell surface molecules. *Science*, 200(4342):618–627, 1978.

[3] Robert B Best, Susan B Fowler, Jose L Toca Herrera, Annette Steward, Emanuele Paci, and Jane Clarke. Mechanical unfolding of a titin ig domain: structure of transition state revealed by combining atomic force microscopy, protein engineering and molecular dynamics simulations. *Journal of molecular biology*, 330(4):867–877, 2003.

[4] DP Blair and PH Sydenham. Phase sensitive detection as a means to recover signals buried in noise. *Journal of Physics E: Scientific Instruments*, 8(8):621, 1975.

[5] Alessandro Borgia, Philip M Williams, and Jane Clarke. Single-molecule studies of protein folding. *Annu. Rev. Biochem.*, 77:101–125, 2008.

[6] Carlos Bustamante, John F Marko, Eric D Siggia, and S Smith. Entropic elasticity of λ-phage dna. *Science*, 265(5178):1599–1600, 1994.

[7] Ciro Cecconi, Elizabeth A Shank, Carlos Bustamante, and Susan Marqusee. Direct observation of the three-state folding of a single protein molecule. *Science*, 309(5743):2057–2060, 2005.

[8] Surya Pratap S Deopa, Shatruhan Singh Rajput, Aadarsh Kumar, and Shivprasad Patil. Direct and simultaneous measurement of the stiffness and internal friction of a single folded protein. *The Journal of Physical Chemistry Letters*, 13(40):9473–9479, 2022.

[9] Evan Evans and Ken Ritchie. Dynamic strength of molecular adhesion bonds. *Biophysical journal*, 72(4):1541–1555, 1997.

[10] Thomas E Fisher, Andres F Oberhauser, Mariano Carrion-Vazquez, Piotr E Marszalek, and Julio M Fernandez. The study of protein mechanics with the atomic force microscope. *Trends in biochemical sciences*, 24(10):379–384, 1999.

[11] Ernst-Ludwig Florin, Manfred Radmacher, Bernhard Fleck, and Hermann E Gaub. Atomic force microscope with magnetic force modulation. *Review of Scientific Instruments*, 65(3):639–643, 1994.

[12] Susan B Fowler and Jane Clarke. Mapping the folding pathway of an immunoglobulin domain: structural detail from phi value analysis and movement of the transition state. *Structure*, 9(5):355–366, 2001.

[13] Jeffrey L Hutter and John Bechhoefer. Calibration of atomic-force microscope tips. *Review of scientific instruments*, 64(7):1868–1873, 1993.

[14] Daniel Kiracofe and Arvind Raman. Quantitative force and dissipation measurements in liquids using piezo-excited atomic force microscopy: a unifying theory. *Nanotechnology*, 22(48):485502, 2011.

[15] Siegfried Labeit, Mathias Gautel, Anne Lakey, and John Trinick. Towards a molecular understanding of titin. *The EMBO journal*, 11(5):1711–1716, 1992.

[16] YZ Liu, SH Leuba, and Stuart Lindsay. Relationship between stiffness and force in single molecule pulling experiments. *Langmuir*, 15(24):8547–8548, 1999.

[17] John F Marko and Eric D Siggia. Stretching dna. *Macromolecules*, 28(26):8759–8770, 1995.

[18] Keir C Neuman and Attila Nagy. Single-molecule force spectroscopy: optical tweezers, magnetic tweezers and atomic force microscopy. *Nature methods*, 5(6):491–505, 2008.

[19] SJ O'Shea. Comment on "oscillatory dissipation of a simple confined liquid". *Physical review letters*, 97(17):179601, 2006.

[20] Shivprasad Patil, George Matei, Hang Dong, Peter M Hoffmann, Mustafa Karaköse, and Ahmet Oral. A highly sensitive atomic force microscope for linear measurements of molecular forces in liquids. *Review of Scientific Instruments*, 76(10), 2005.

[21] Shatruhan Singh Rajput, Surya Pratap S Deopa, VJ Ajith, Sukrut C Kamerkar, and Shivprasad Patil. Validity of point-mass model in off-resonance dynamic atomic force microscopy. *Nanotechnology*, 32(40):405702, 2021.

[22] Felix Rico, Laura Gonzalez, Ignacio Casuso, Manel Puig-Vidal, and Simon Scheuring. High-speed force spectroscopy unfolds titin at the velocity of molecular dynamics simulations. *Science*, 342(6159):741–743, 2013.

[23] Annafrancesca Rigato, Atsushi Miyagi, Simon Scheuring, and Felix Rico. High-frequency microrheology reveals cytoskeleton dynamics in living cells. *Nature physics*, 13(8):771–775, 2017.

[24] Michael Schlierf and Matthias Rief. Temperature softening of a protein in single-molecule experiments. *Journal of molecular biology*, 354(2):497–503, 2005.

[25] Fidan Sumbul, Nahid Hassanpour, Jorge Rodriguez-Ramos, and Felix Rico. One-step calibration of afm in liquid. *Frontiers in Physics*, 8:301, 2020.

[26] Fidan Sumbul, Arin Marchesi, Hirohide Takahashi, Simon Scheuring, and Felix Rico. High-speed force spectroscopy for single protein unfolding. *Nanoscale Imaging: Methods and Protocols*, pages 243–264, 2018.

[27] Fidan Sumbul and Felix Rico. Single-molecule force spectroscopy: experiments, analysis, and simulations. *Atomic Force Microscopy: Methods and Protocols*, pages 163–189, 2019.

[28] N Umeda, S Ishizaki, and H Uwai. Scanning attractive force microscope using photothermal vibration. *Journal of Vacuum Science & Technology B: Microelectronics and Nanometer Structures Processing, Measurement, and Phenomena*, 9(2):1318–1322, 1991.

[29] Yong Wang and Giovanni Zocchi. The folded protein as a viscoelastic solid. *Europhysics Letters*, 96(1):18003, 2011.

[30] Yong Wang and Giovanni Zocchi. Viscoelastic transition and yield strain of the folded protein. *PLoS One*, 6(12):e28097, 2011.

[31] Xin Xu and Arvind Raman. Comparative dynamics of magnetically, acoustically, and brownian motion driven microcantilevers in liquids. *Journal of Applied Physics*, 102(3), 2007.